# THE IMPACT OF IGNORED NEGLIGIBLE LOSSES IN ENGINEERING DESIGN: AERODYNAMIC DRAG ON ET425M HIGH SPEED TRAIN AS STUDY CASE

MUHAMMAD HAFIZUDDIN BIN ZAINAL ABIDIN

SUBMITTED TO THE

FACULTY OF ENGINEERING

UNIVERSITY OF MALAYA, IN PARTIAL

FULFILMENT OF THE REQUIREMENTS FOR

THE DEGREE OF MASTER OF ENGINEERING IN MECHANICAL

2019

**UNIVERSITY OF MALAYA**

**ORIGINAL LITERARY WORK DECLARATION**

Name of Candidate: MUHAMMAD HAFIZUDDIN BIN ZAINAL ABIDIN

Matric No: KQK170005

Name of Degree: MASTER OF MECHANICAL ENGINEERING

Title of Project Paper/Research Report/Dissertation/Thesis ("this Work"):

THE IMPACT OF IGNORED NEGLIGIBLE LOSSES IN ENGINEERING DESIGN: AERODYNAMIC DRAG ON ET425M HIGH SPEED TRAIN AS STUDY CASE

Field of Study: MECHANICAL ENGINEERING

I do solemnly and sincerely declare that:

(1) I am the sole author/writer of this Work;
(2) This Work is original;
(3) Any use of any work in which copyright exists was done by way of fair dealing and for permitted purposes and any excerpt or extract from, or reference to or reproduction of any copyright work has been disclosed expressly and sufficiently and the title of the Work and its authorship have been acknowledged in this Work;
(4) I do not have any actual knowledge nor do I ought reasonably to know that the making of this work constitutes an infringement of any copyright work;
(5) I hereby assign all and every rights in the copyright to this Work to the University of Malaya ("UM"), who henceforth shall be owner of the copyright in this Work and that any reproduction or use in any form or by any means whatsoever is prohibited without the written consent of UM having been first had and obtained;
(6) I am fully aware that if in the course of making this Work I have infringed any copyright whether intentionally or otherwise, I may be subject to legal action or any other action as may be determined by UM.

Candidate's Signature Date:

Subscribed and solemnly declared before,

Witness's Signature Date:

Name:

Designation

# THE IMPACT OF IGNORED NEGLIGIBLE LOSSES IN ENGINEERING DESIGN: AERODYNAMIC DRAG ON ET425M HIGH SPEED TRAIN AS STUDY CASE


## ABSTRACT

ET425M high speed train built by Siemens for Express Rail Link to operate between Kuala Lumpur Sentral station to Kuala Lumpur International Airport. ET425M air conditioning units that installed on the roof section not incorporated with any air deflector design to mitigate additional air resistance. The additional drag resistance adds to train motion resistance that leads to higher traction effort thus conclude to additional power consumption. With using Ansys Fluent solver, the drag force, drag coefficient and max pressure acts on the original air conditioning unit design of ET425M is determined and compared with introduction of air deflector with various angle. With introduction of air deflector with angle of 20 degree, the drag force showed reduction of 27% reduction of drag force, 29% reduction of drag coefficient and 46% reduction of max pressure when train simulated moving at train velocity of 160Km/h. With using approximation and assumption method by comparing the difference of tractive effort to determine the relationship between reductions of air resistance with power consumption, a reduction of 3% is achieved which translated to saving of RM 7,458,674 for operation of 30 years with current train operation frequency.



Keywords: Drag force, Air deflector, Tractive effort, Power consumption

# KESAN KEHILANGAN YANG BOLEH DIABAIKAN DALAM REKAAN KEJURUTERAAN: DAYA SERET YANG DIALAMI KERETAPI LAJU ET425M SEBAGAI KES KAJIAN


## ABSTRAK

Keretapi laju ET425M dibina oleh Siemens untuk Express Rail Link bagi operasi perkhidmatan keretapi antara Stesen Sentral Kuala Lumpur dan Lapangan Terbang Antrabangsa Kuala Lumpur.Unit penghawa dingin ET425M yang dipasang di bahagian bumbung tidak direka dengan pengawal udara untuk mengawal pertambahan rintangan udara. Pertambahan rintangan udara menambah rintangan keretapi untuk bergerak yang membawa kepada pertambahan kepada penambahan daya tarikan yang membawa kepada pertambahan kos pengunaan elektrik. Dengan menggunakan simulasi Ansys Fluent, daya seret, pekali seret dan tekanan maksima yang dialami oleh rekaan asal unit penghawa dingin ET425M ditentukan dan dibandingkan dengan pengenalan pengawal udara pelbagai darjah kecerunan.Dengan pengenalan pengawal udara kecerunan 20 darjah, daya seret dikurangkan kepada 27%, pengurangan pekali seret sebanyak 29% dan 46% pengurangan tekanan maksima apabila disimulasikan dengan kelajuan keretapi 160Km/h.Dengan menggunakan kaedah penghampiran dan andaian bagi membandingkan daya tarikan untuk menentukan hubungan pengurangan rintangan udara dengan pengunaan elektrik, pengurangan sebanyak 3% telah dicapai yang mebawa kepada penjimatan sebanyak RM 7,458,674 untuk operasi selama 30 tahun dengan kadar operasi sediada.



Kata kunci: Daya seretan, Pengawal udara, Daya tarikan, Pegunaan tenaga

**ACKNOWLEDGEMENTS**

A very a high gratitude to my maker which have guided me, given me wisdom and strength to complete this research project.

Very special thanks to my supervisor, Associate Professor. Dr. Ir. Nik Ghazali which have provided me beneficial advices and guidance in course to complete this project.

A humble appreciation to Express Rail Link that provide me insight and info that help me understand ET425M design and Express Rail Link train operation.

Last but not least, my wife and fellow classmates that have contributed to completion of this research project directly or indirectly.

**TABLE OF CONTENT**

## LIST OF FIGURES

## LIST OF TABLES

## LIST OF SYMBOLS AND ABBREVIATIONS

| | | |
|---|---|---|
| Cd | - | Drag coefficient |
| % | - | Percentage |
| CFD | - | Computational fluid dynamic |
| DOE | - | Design of experiment |
| ERL | - | Express Rail Link |

## LIST OF APPENDICES

# 1. INTRODUCTION

The expected negligible losses found during design phase for any engineering works usually ignored as it possesses insignificant impact on the final product in term of reliability, safety and operationalbility. This research paper focuses on impact of the ignored additional aerodynamic resistance. The air conditioning unit installed on roof section of ET425M high speed train was found been designed in typical rectangle box unit with no features to mitigate aerodynamic resistance. As the dimension of the air conditioning unit is relative small when compared to dimension of the train, it believed carries insignificant additional aerodynamic resistance which translate to insignificant additional tractive effort which equal to insignificant additional power consumption. However, for an engineering design that expected to be operational for 30 years such as ET425M high speed train, it expected the additional power consumption shall contribute significant additional operation cost. By using CFD simulation through Ansys Fluent software, the aerodynamic drag of the air conditioning unit is studied and the relationship to additional power consumption shall be established.

# 2. LITERATURE REVIEW

## 2.1. Engineering Design Process

Designing stage is a vital stage that which contributes significantly to the final product or engineering work during operation stage. Typically engineering design begins with setting the objectives of the design. For an example, a car must be designed to exceed top speed of 250Km/h with breaking time of 5 seconds. The design works will focus on how to achieve the top speed with the expected breaking time. However, the car may require a very delicate power train design and braking system that may very costly but cost saving was not the objective of the design. Defining the problem to achieve the design objectives is a very first crucial step (Khandani, 2005). For the example of the car, achieving top speed of 250Km/h with breaking speed of 5 seconds is the objectives. Therefore, defining all problems that prevent the car from achieving it is the utmost priority. Any other problem that may arise during the process such as high fuel consumption, high rate wear & tear of the brakes and short life span of the engine due to expectation to deliver enormous amount of power is deliberately been ignored.

However, all arise problem may be taken to account as it been discovered during designing stage and carries significant impact during operation stage. As the impact of the problem is known, it worth the effort to eliminate or reducing it during engineering design process. Therefore, it is important for engineers to understand the impact of the problem onto the design.

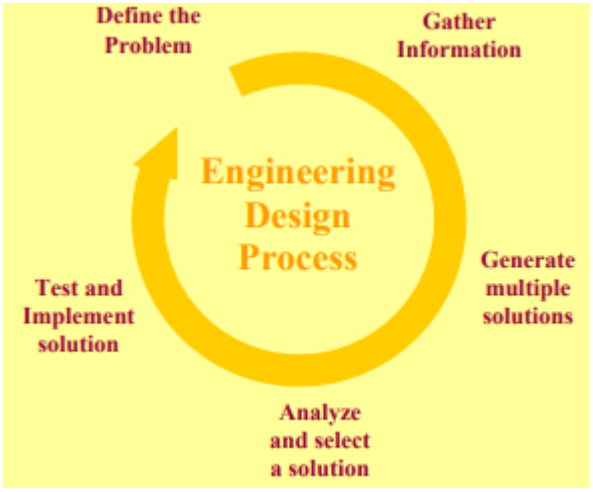


Figure 2.1: Engineering design process (Khandani, 2005).

## 2.2. Aerodynamic Drag

General understanding of aerodynamic is the behaviour of air flows around an object. Anything moving is subject to aerodynamic forces which govern by Newton 3rd law and Bernoulli's principle. Aerodynamic forces which usually divided into two components which is drag force and lift force. These two components are important parameters in dynamic engineering design. Drag force is an opposing force of an object. Drag force is derivation from Buckingham $\pi$ theorem (Maxemow, 2009) which leads to drag force function which dependant to velocity, fluid density, affected area and viscosity which generally expressed in as follows equation:

$$FD = 1/2pv2CdA$$

Drag coefficient is used to quantify the drag resistance exerted by an object when moves in fluid regardless compressible or incompressible fluid. Drag coefficient is closely related with affected surface area and shape of the object. Drag coefficient is contributed by these both type of fluid dynamic drag which is skin friction and form drag. Skin friction is interaction between fluid flow and the surface area of the object and form drag is associated with shape of the object. Drag coefficient is used to measure effectiveness of an object in

opposing air resistance during motion (Heisler, 2002). Low drag coefficient implies the object move freely in fluid and high drag coefficient translate to difficulty to move in fluid as high opposing force to the motion.

Table 2.1: Typical drag coefficient of vehicles (Heinz, 2002).

| Vehicle type drag coefficient, CD | |
|---|---|
| Saloon car | 0.22-0.4 |
| Sports car | 0.28-0.4 |
| Light van | 0.35-0.5 |
| Busses and coaches | 0.4-0.8 |
| Articulated trucks | 0.55-0.8 |
| Ridged trucks and draw bar trailer | 0.7-0.9 |

Drag coefficient is a variation of function of speed, object shape, fluid density, direction of the motion and fluid viscosity and drag coefficient is not a constant. Shape of an object and Reynolds number contribute greatly on drag coefficient. An experiment conducted (Gemba, 2007) to understand the impact of shapes and Reynolds number on drag.

Below are shapes used as test specimen.

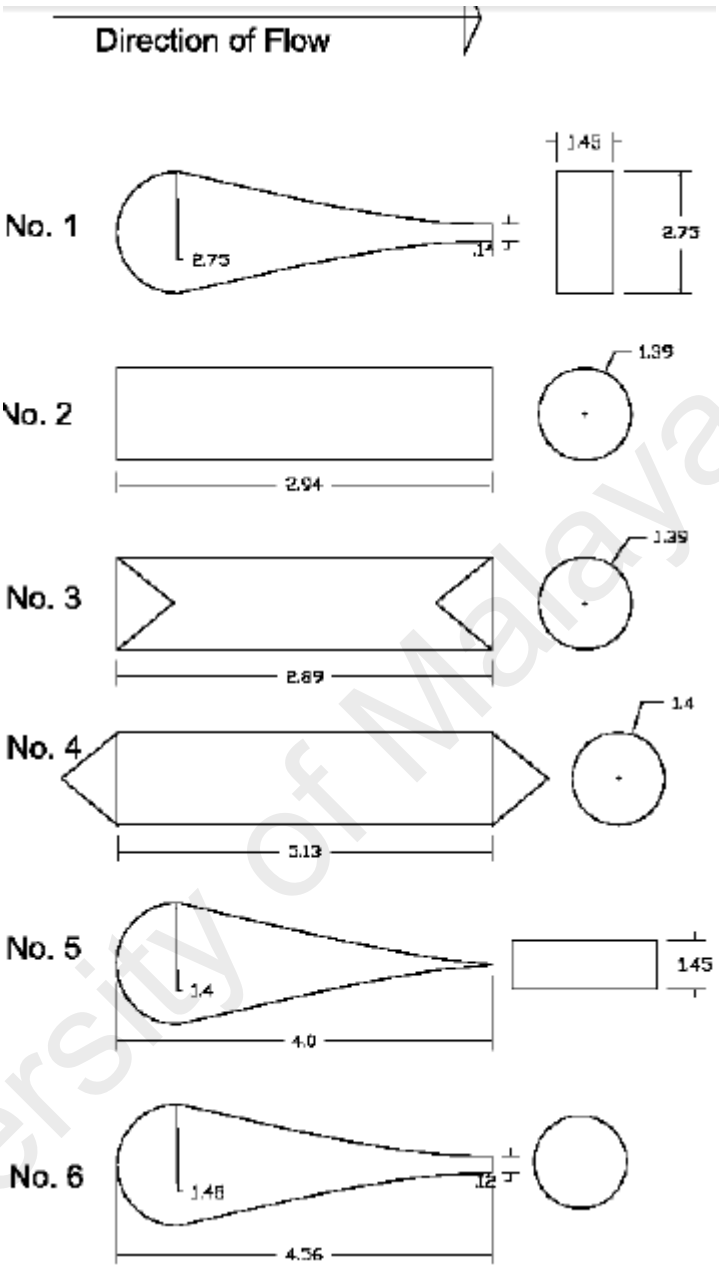


Figure 2.2: Tested objects, dimensions: inch

Drag forces for all test specimens increased as Reynolds number and stream velocity build up. The test specimen that clearly possesses good aerodynamic flow features such as 4, 5, and 6 showed the lowest drag. Test specimen no 6 deemed as the best aerodynamic shape as it showed almost 50% less drag if compared to test specimen no 3, 2 and 1 (Gemba, 2007).

## 2.3. Design Optimization for Drag Reduction

As generally understood that shape has significant impact in contributing the unwanted drag resistance that not contributing to dynamic stability of an object. Various studies have been conducted to optimize the design to reduce drag coefficient hence reducing the drag force. An object shall be designed with various method of shape optimization to obtain the most wanted goal which resulted with lowest drag coefficient. A simple rounding the sharp corners, front and rear of an object have resulted of 40% of drag reduction (Conner, 2017).

Figure 2.3: A standard passenger van modified to understand the impact of shape optimization with drag reduction

Design optimization for drag reduction usually been looked point of views but not limited to streamlining airflow, covering exposed underbody structure and extent of wake and flow separation. Taguchi method is a method of design optimization that proved design of experiments (DOE) should be use if quality of manufactured output is hope to achieve (Abdellah, 2015). A good aerodynamic shape is a shape that delay flow separation, creates less wake turbulence and eliminate as much numbers of stagnation point or a point where the flow velocity is zero.

## 2.4. Air Deflector to Reduce Drag

Frontal area of an object is the first point of contact to experience drag resistance. A pure sharp square object frontal area has tendency to possess high numbers of stagnation point thus creating high drag resistance. A streamlined, blunted sharp edge possesses lower numbers of stagnation points as air flows more freely around it. A semi-trailer truck without an air deflector installed on the roof of the driving cab showed a drag coefficient approximately of 0.80 when a similar semi-trailer truck installed with air deflector showed approximate drag coefficient of 0.67 when both simulated moving at speed of 40 Km/h (Chowdhury et al ,2013).

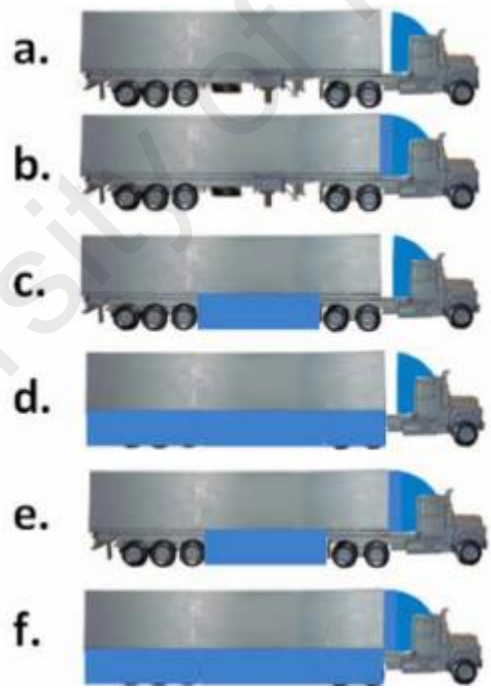


Figure 2.4: Semi trailer test model installed with various type of air deflector (Chowdhury et al, 2013).

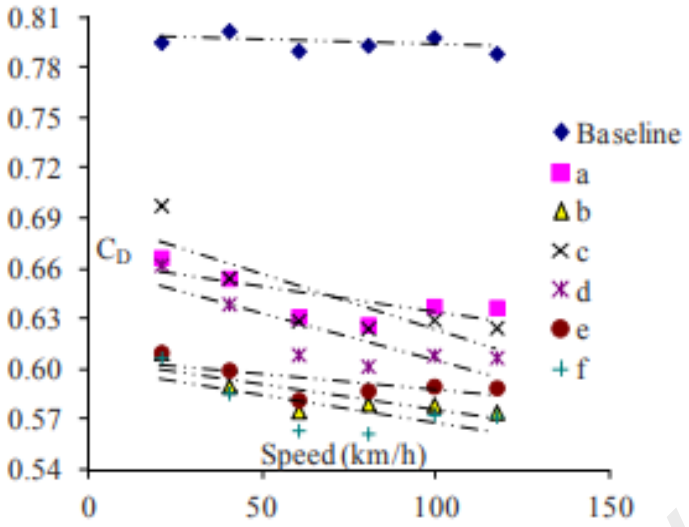


Figure 2.5: Comparison of drag coefficient (Chowdhury et al ,2013).

As illustrated in figure 2.5, air deflector does imply a significant role in reducing drag coefficient hence reducing drag resistance. The tested air deflector managed to mitigate the impact of wake turbulence and unchecked stagnation points.

Various studies of optimization of air deflector to reduce drag resistance have been conducted as it delivered favourable outcome from time to time. A different study showed optimization of air deflector managed to reduce initial drag of 2050N to 1688.453N which is translated to reduction of resistance of 17.6% (Ramesh et al, 2017).

Table 2.2: Drag force for reduction by optimization air deflector (Ramesh et al, 2017)

| Angle of wind deflect-or | Drag force (1m) in N | Drag force (1.25m) in N | Drag force (1.5m) in N | Drag force (1.75m) in N |
|---|---|---|---|---|
| 30 | 1958.764 | 1866.244 | 1858.655 | 1857 |
| 35 | | 1844.62 | 1802.042 | 1820 |
| 40 | 1860.063 | 1819.701 | 1800.983 | 1787.369 |
| 45 | 1846.176 | 1801.363 | 1695.266 | 1688.453 |
| 50 | 1824.922 | 1763.86 | 1711.011 | 1747.998 |
| 60 | 1736.566 | 1734.19 | 1808.906 | 1868.839 |
| 70 | 1768.95 | 1812.826 | 1884.662 | 1981.503 |

## 2.5. The Impact of Reduced Drag

To move an object to motion, energy must have to be generated to overcome the resistance force. Lesser resistance hence less energy is required to move an object into a desired speed. Typical semi-trailer truck utilized energy generated from piston engines that dependant on burning of fossil fuel and a typical high speed train or normal metro train, utilized energy from traction motor that dependant on electrical power supply to established a forward motion and overcome resistance force. A reduction in drag resistance will result in lesser energy consumption. A reduction of 37% of aerodynamic resistance resulted to 6% reduction of fuel consumption with introduction of new design of air spoiler or air deflector (Cihan, 2017).

## 2.6. Aerodynamic Drag of Train

All featured design of train regardless traction power dependant or diesel power dependant to generate a forward motion is subjected to motion resistance. Two typical resistance of a train which categories into inherent resistance and incidental resistance. Train resistance usually better is understood by Davis formula (Newcastle, 2017). The formula translated to as follows empirical illustration:

$$R=A+BV+CDV2$$

Which are:

R= Total train resistance force
A= Rolling resistance
B= A train resistant coefficient dependant on train speed
C=Streamlining coefficient
D=Aerodynamic coefficient which often combined with C
V= Train velocity

Table 2.3: Summary of A, B, C&D of Davis formula (Newcastle, 2017)

| A | B | C & D |
|---|---|---|
| Journal / Roller Bearing Resistance | Flange friction | Head-end wind pressure |
| Rolling resistance | Flange impact | Skin friction on the side of the train |
| Track resistance | Rolling resistance wheel/rail | Rear drag |
| | Wave action of the rail | Turbulence between cars |
| | | Yaw angle of wind tunnels |

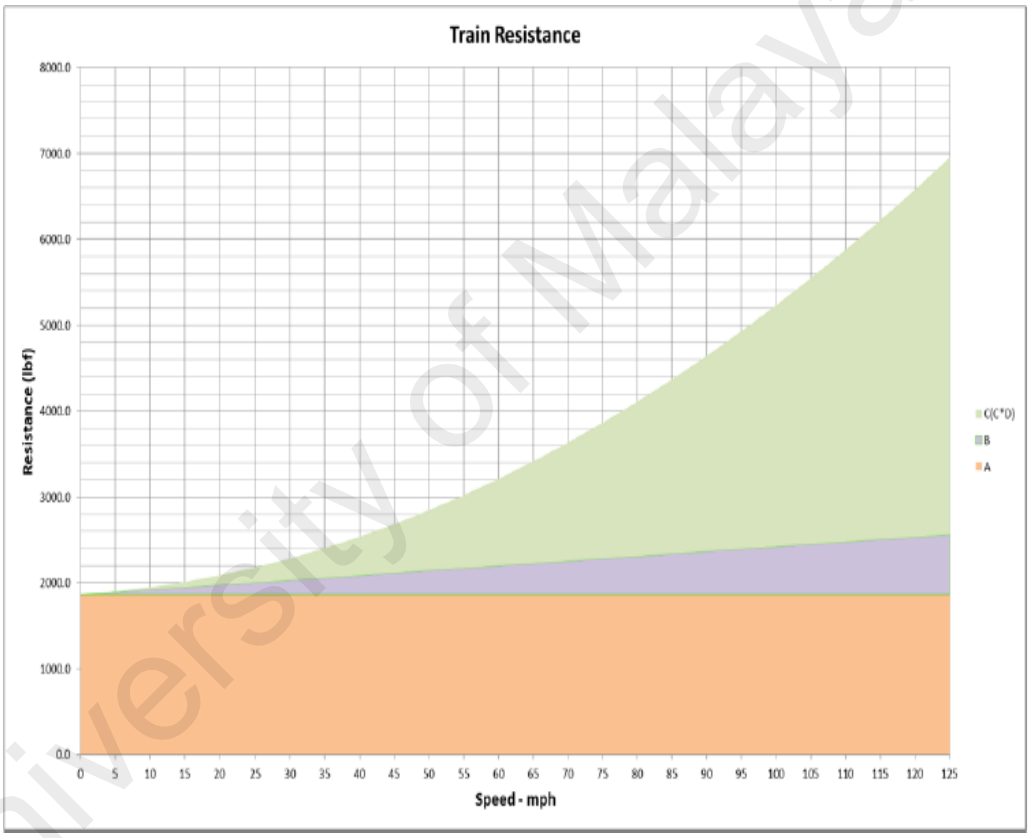


Figure 2.6: Impact of each Davis coefficients on resistance force (Newcastle, 2017).

As illustrated by figure 2.6, as velocity of the train increase, resistance force contributed by coefficient A remain constant and resistance force contributed by coefficient B also have the same contributing factor as coefficient A.

However, resistance force contributed by coefficient C & D increase as velocity of the train increase. Resistance force experienced by a train due to factor of form drag worth to be study further.

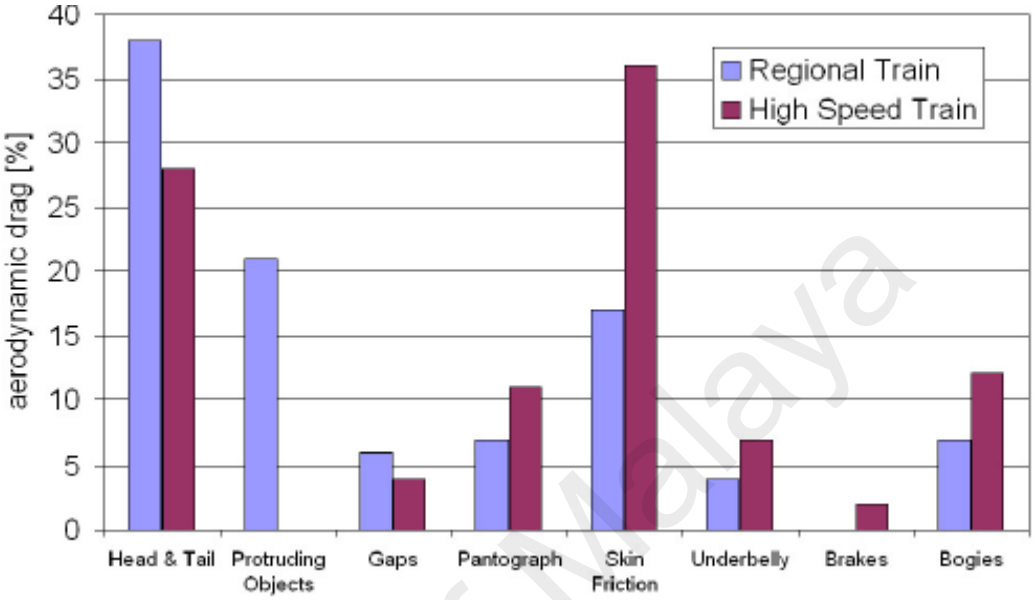


Figure 2.7: Drag distribution of a high speed and regional train (Orellano & Sperling, 2007).

As illustrated by figure 2.7 is typical drag distribution exerted by a train, an actual drag distribution is highly depending on actual train design and motion scenario. Protruding objects such as air conditioning unit, telecommunication antenna, pantograph or any other equipment which are protruding or installed on the top roof section are the common source of drag resistance if compared to a train design that conceals all protruding equipment (Orellano & Sperling, 2007).

## 2.7. Impact of Reduced Train Drag Resistance

As the source of contributing drag resistance have been understood that leads to various study to understand the impact of the drag resistance to energy consumption regardless diesel powered train or electrical powered train.

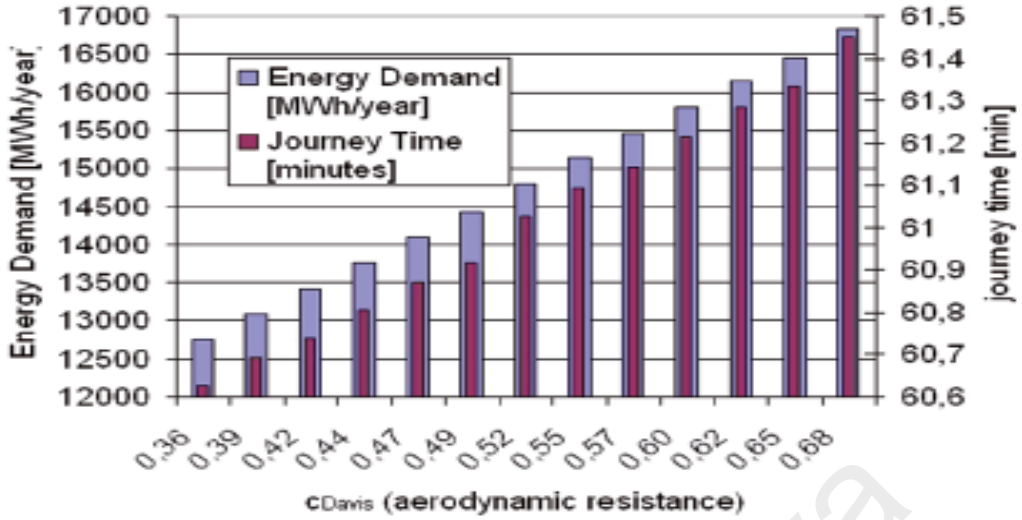


Figure 2.8: Impact of drag resistance on energy demand (Orellano & Sperling, 2007).

The study conducted that illustrated in figure 8 shows that with improvement of train design that focused on reduction of drag resistance contributed significantly to reduction in energy demand. Potential possesses by drag reduction alone to reduce energy demand in typical journey of a train is huge and estimated to be in range of 20-25% and will lead to reduction of 6-8% of energy demand hence lead to saving of about 200MWh/year per train (Orellano & Sperling, 2007).

A different study conducted to understand the impact of drag reduction of diesel fuel powered rolling stock or train type (Paul et al, 2007). The study amplified on protruding design relationship with consumption of diesel fuel. With just removing the protruding objects out from the design, it leads to reduction of 8% in demand for diesel fuel per 1600 kilometres when moving at speed of 65 Km/h at normal level route.

## 2.8. ET425M High Speed Train

ET425M built by Siemens to operate train service from Kuala Lumpur Sentral Station (KL Sentral) to Kuala Lumpur International Airport (KLIA). The train dedicatedly designed for Express Rail Link that main objective to achieve

travelling time lesser than 28 minutes from KL Sentral to KLIA and denoted as fastest train in Malaysia.ET425M is electrically powered and consist of four-car train with total length 68 metre with maximum load of approximate 136 tonnes. Design philosophy of ET425M is to possess high power performance with low energy consumption and expected to have design life of 30 years. Express Rail Link runs 237 trips daily (ERL, personal communication, 16 June 2019).

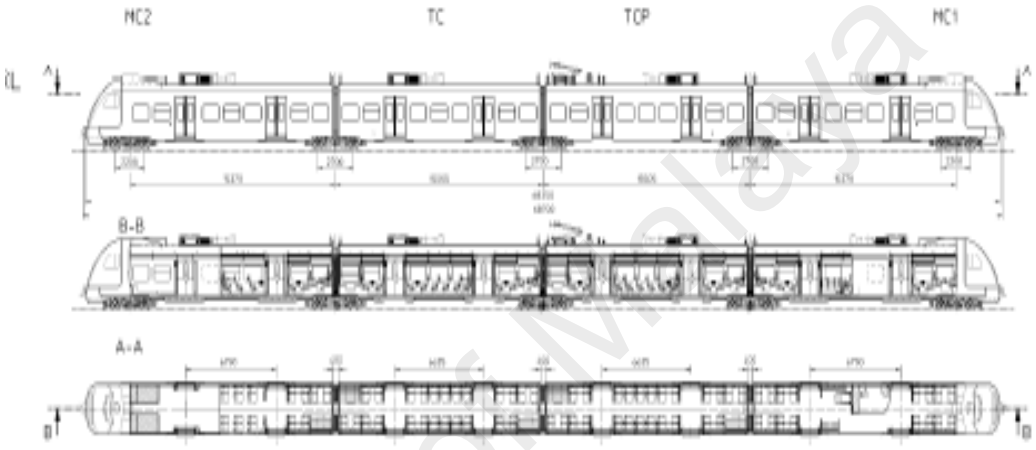


Figure 2.9: Overview drawing of ET425M

Table 2.4: Dimensions of ET425M

| | |
|---|---|
| Length over coupler face of 4-car unit | 68,700 mm |
| Length over coupler face of Motor Car | 18,845 mm |
| Length over coupler face of Trailer Car | 15,505 mm |
| | |
| Overall width, nominal | 2,840 mm |
| | |
| Height of pantograph (down) above rail level (nominal, unloaden) | 4,225 mm |
| Height of floor above rail level (nominal, unloaden, w/o flooring) | 798 mm |
| Height of seating area ceiling above floor (nominal) | 2,200 mm |
| Height of vestibule ceiling above floor (nominal) | 2,310 mm |
| | |
| | |
| Nominal clear width of entrance door (w/o hand rails) | 1,300 mm |
| Nominal clear height of entrance door | 1,980 mm |
| Minimum gangway aisle width at the bottom | 715 mm |
| Nominal aisle width at end walls | 690 mm |
| Nominal aisle width at seat boxes (knee height) | 616 mm |
| Minimum aisle width at coupler area over seats level | 2,000 mm |
| Distance between bogie centres Motor Car | 15,370 mm |
| Distance between bogie centres Trailer Car | 15,505 mm |
| | |
| Height of coupler head centre above top of rail (tare) | 1,030 mm |
| | |
| Maximum wheel diameter new | 850 mm |
| Minimum wheel diameter worn | 780 mm |

Table 2.5: ET425M nominal performance

| | |
|---|---|
| Maximum design speed | 176 km/h |
| Maximum service speed | 160 km/h |
| Installed power of traction equipment | 1.8 MW at rim |
| Power during electrical braking | 2.0 MW at rim |
| Starting effort | 150 kN |
| Constant power range | from v > 43.2 km/h |
| Catenary voltage (rated voltage) | 25 kV |
| Frequency | 50 Hz |
| Psophometric current | 3 A (approx.), normal operation condition |
| Power factor | ~ 1 at 25 kV, controlled |
| Range of full power | 23 kV ... 27,5 kV |
| Range of power reduction | 19 kV ... 23 kV |
| Max. starting acceleration | 1.0 m/s² |
| Max. electrical deceleration | -0.9 m/s² |
| Max. emergency deceleration (friction brake only) | -1.16 m/s² |

### 2.8.1. ET425M Energy Consumption

ET425M energy demands supplied by tractive power generated by traction motor. As design philosophy of ET425 is high performance with less energy consumption. That philosophy been achieved by focusing on optimizing weight and regenerative braking or reused generated electricity during braking. Figure shows driving resistance and tractive effort of ET425M.

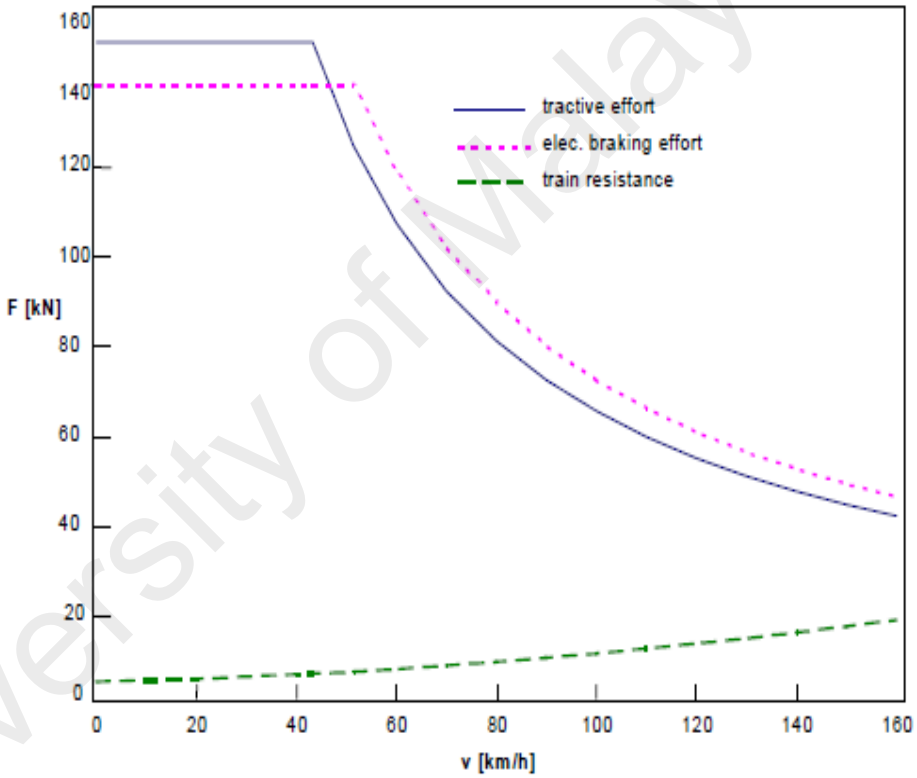


Figure 2.10: ET425M driving resistance and tractive effort

The figure illustrated driving resistance and tractive effort based on adhesion coefficient of 0.17 (starting) and 0.16 (braking) with fully loaded passengers and half worn wheel (Siemens, 2000). It can be interpreted that maximum train air resistance is approximately 20,000 N when operating at maximum commercial speed.

Energy consumption recorded by a trip by ET425M journey from Kuala Lumpur Sentral Station (KL Sentral) to Kuala Lumpur International Airport (KLIA) is at 279KWh (ERL, personal communication, 16 June 2019)

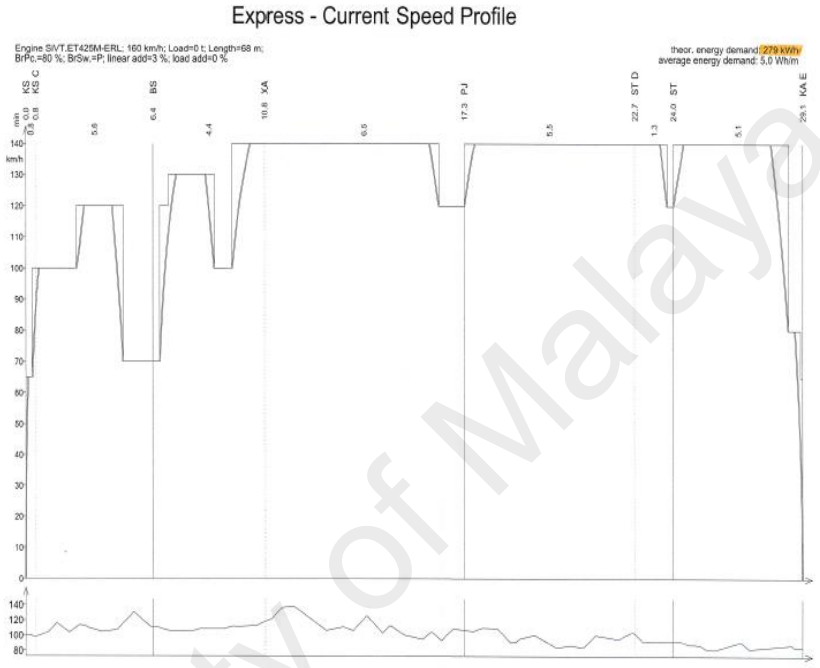


Figure 2.11: ET425M energy consumption for a single trip

## 2.9. Train Energy Consumption Prediction Method

To estimate and predict train power consumption per trip requires a very specified and accurate data such as train velocity, total running time, and corresponding tractive effort with braking force. A train performance simulator is a common simulation used in the industry to analyse all the data to establish the relationship between each parameter. Train performance simulation conducted by TMG International Consultant showed reduction of 13.7 % reduction in energy consumption by time table optimization alone (Jong & Chang, 2005).

## 2.10. Computational Fluid Dynamic Simulation for Drag Force

Computational fluid dynamic is a discipline to simulate and predict behaviour of the design during operation stage interaction with fluid flows using numerical analysis. The data structure collected helps engineers to improve the design and identified flaws that may require for redesign especially involving drag resistance and improving drag coefficient.

A study conducted by (Joung et al, 2014) to verify the result obtained by via CFD analysis to predict drag force and thrust power. The conclusion showed the experimental result is reliable to predict behaviour of concept early stage on their design process.

# 3. METHODOLOGY

## 3.1. Introduction

This research project scope focused on defining the drag force, drag coefficient and max pressure of original ET425M roof top air conditioning design and compared with same parameter of the suggested new designs. Standard K-epsilon is used as viscous model with as follow governing equations:

For turbulent kinetic energy $k$

$$\frac{\partial}{\partial t}(\rho k) + \frac{\partial}{\partial x_i}(\rho k u_i) = \frac{\partial}{\partial x_j}\left[\left(\mu + \frac{\mu_t}{\sigma_k}\right)\frac{\partial k}{\partial x_j}\right] + P_k + P_b - \rho\epsilon - Y_M + S_k$$

For dissipation $\epsilon$

$$\frac{\partial}{\partial t}(\rho\epsilon) + \frac{\partial}{\partial x_i}(\rho\epsilon u_i) = \frac{\partial}{\partial x_j}\left[\left(\mu + \frac{\mu_t}{\sigma_\epsilon}\right)\frac{\partial \epsilon}{\partial x_j}\right] + C_{1\epsilon}\frac{\epsilon}{k}(P_k + C_{3\epsilon}P_b) - C_{2\epsilon}\rho\frac{\epsilon^2}{k} + S_\epsilon$$

Figure 3.1: Standard K-epsilon governing equations

## 3.2. Original Design

Each original ET425M air conditioning unit design is sketched using Design Modeller software with dimension of the original design.ET425M have 4 air conditioning units installed on the roof section. The dimension of the original design is as follows:

Table 3.1: ET425M air conditioning unit dimension

| | |
|---|---|
| **Height:** | 0.5 m |
| **Width:** | 1.8 m |
| **Length:** | 2.85 m |

Table 3.2: ET425M roof section dimension

| | |
|---|---|
| **Width:** | 3.0 m |
| **Length:** | 60.0 m |

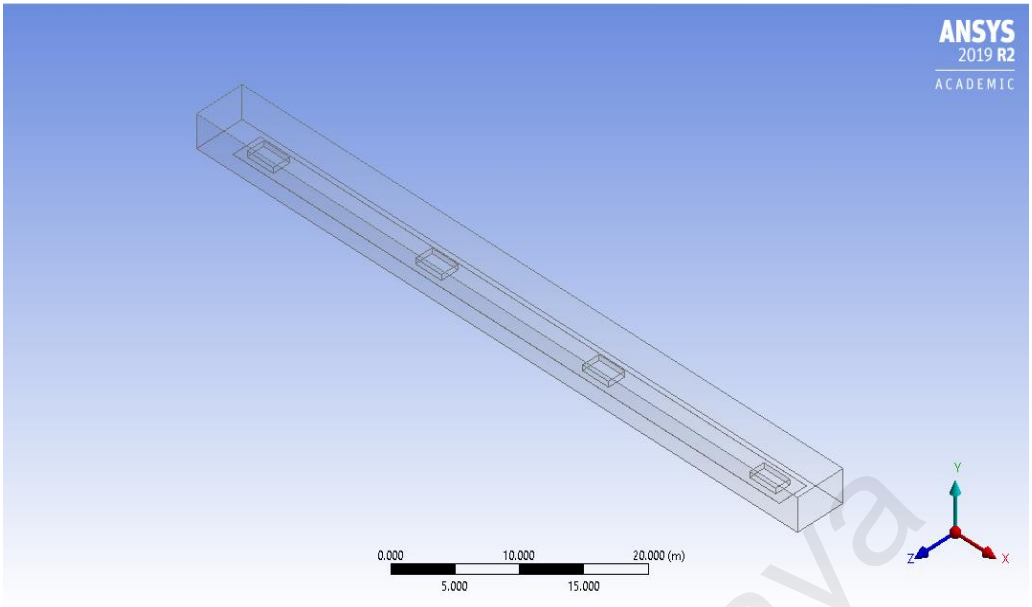


Figure 3.2: Geometry of roof section of ET425M with air conditioning units only

Drag force, drag coefficient and max pressure of ET425M original air conditioning unit is defined using ANSYS FLUENT 19 R12 ACADEMIC solver. The parameters used are as follows:

Table 3.3: Mesh details of original design

| | |
|---|---|
| **Element order:** | Program controlled |
| **Element size:** | 0.5 m |
| **Nodes:** | 94019 |
| **Elements:** | 60963 |

Table 3.4: Viscous model details

| | |
|---|---|
| **Model:** | Standard K-epsilon (2eqn) |
| **Cmu** | 0.09 |
| **C1-epsilon:** | 1.44 |
| **C2-epsilon:** | 1.92 |
| **TKE prandtl number:** | 1 |
| **TDR prandtl number:** | 1.3 |

Table 3.5: Original design reference values

| | |
|---|---|
| **Projected area:** | 5.6 m2 |
| **Air density:** | 1.225 kg/m3 |
| **Enthalpy:** | 0 j/kg |
| **Pressure:** | 0 Pascal |
| **Temperature:** | 288.16 k |
| **Viscosity:** | 1.7894e-5 |
| **Ratio of specific heat:** | 1.4 |

Original ET425M air conditioning design is simulated using as per defined parameters with different inlet velocity of 160Km/h, 140Km/h, 120Km/h and 100Km/h with initial set iteration of 500 or until converged. Drag force, drag coefficient and max pressure for each inlet velocity are compared.

## 3.3. Suggested Designs

With reference to original ET425 air conditioning design, suggested new designs are each air conditioning unit is incorporated with air deflector with various different angles.

Table 3.6: New design air deflector angle

| Model | Air deflector angle (degree) |
|---|---|
| A | 40° |
| B | 30° |
| C | 20° |

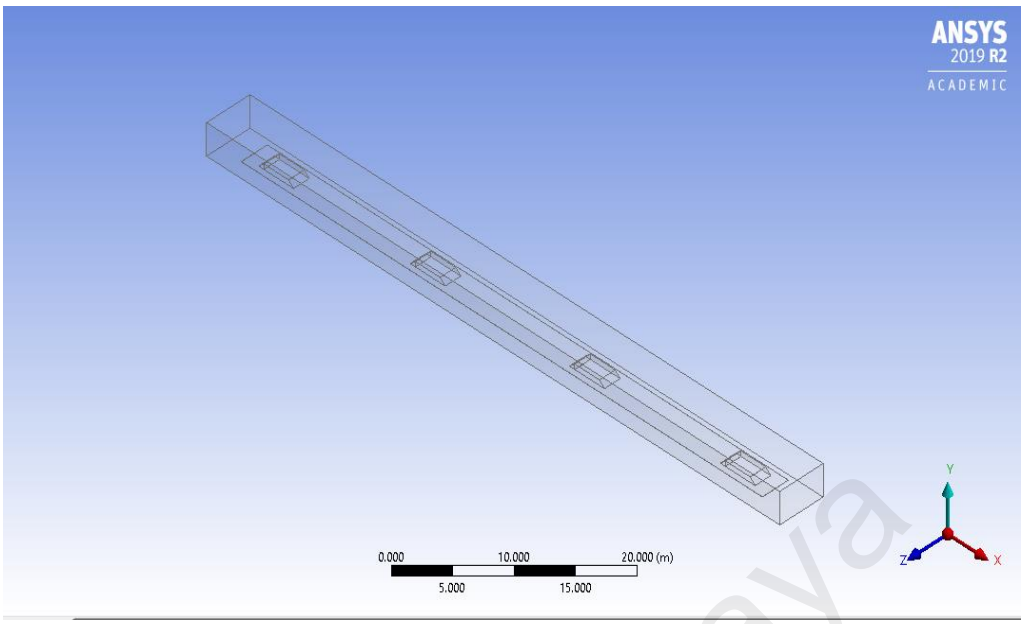


Figure 3.3: Geometry of roof section of ET425M with air conditioning units incorporated with air deflector

Drag force, drag coefficient and max pressure of ET425M new air conditioning unit is defined using ANSYS FLUENT 19 R12 ACADEMIC solver. The parameters used are as follows:

Table 3.7: Model A mesh details

| | |
|---|---|
| **Element order:** | Program controlled |
| **Element size:** | 0.5 m |
| **Nodes:** | 94019 |
| **Elements:** | 60963 |

Model A design is simulated using as per defined parameters as original design with different inlet velocity of 160Km/h, 140Km/h, 120Km/h and 100Km/h with initial set iteration of 500 or until converged. Drag force, drag coefficient and max pressure for each inlet velocity are compared.

Table 3.8: Model B mesh details

| | |
|---|---|
| **Element order:** | Program controlled |
| **Element size:** | 0.5 m |
| **Nodes:** | 94019 |
| **Elements:** | 60963 |

Model B design is simulated using as per defined parameters as original design with different inlet velocity of 160Km/h, 140Km/h, 120Km/h and 100Km/h with initial set iteration of 500 or until converged. Drag force, drag coefficient and max pressure for each inlet velocity are compared.

Table 3.9: Model C mesh details

| | |
|---|---|
| **Element order:** | Program controlled |
| **Element size:** | 0.5 m |
| **Nodes:** | 94019 |
| **Elements:** | 60963 |

Model C design is simulated using as per defined parameters as original design with different inlet velocity of 160Km/h, 140Km/h, 120Km/h and 100Km/h with initial set iteration of 500 or until converged. Drag force, drag coefficient and max pressure for each inlet velocity are compared.

## 3.4. Power Consumption

The power consumption of original drag force resistance is compared with drag force of new suggested design. Train power consumption best to be estimated using establish train performance simulation software to anticipate affecting factors of power consumption such starting effort, motion resistance, number of stops, influence of regenerative braking, acceleration, coasting and etc. Majumdar (Jong, 2005) proposes an equation to estimate train power consumption. The equation as follow figure:

$$W_T = \left[\frac{2.725}{0.814}\left(\sum T_A \times d_A + \sum T_B \times d_B\right)\right] + \left[\frac{P_a}{0.964} \times \left(\frac{\sum d_C}{v_C} + \frac{\sum d_D}{v_D}\right)\right] \quad ($$

where $W_T$ =total power energy consumption (kWh)
$T$ =force in tones due to tractive effort (ton)
$d$ =distance traveled in km at that speed range (km)
$P_a$ =power consumption by all auxiliaries (kWh)
$A, B, C, D$ = Acceleration, Balancing, Coasting and Deceleration stage, respectively

Figure 3.4: Majumdar train power consumption equation

However, with missing actual data as suggested by above equation, to establish power consumption of ET425M using above equation is void. Approximate method to determine the power consumption is used with various assumption to establish the understanding of relationship between air resistance of train and power consumption. A very simplified method is used to determine the differential factor of power consumption of original air conditioning unit design and improved new design by focusing on different of traction effort and air resistance.

With assumption of ET425M constant travelling speed of 160Km/h then the tractive effort is 50,000 N (Siemens, 2000). The air resistance generated from ET425M when travelling at 160Km.h is 20,000N and remaining 30,000 N is other motion resistance (Siemens, 2000) and as per defined by (Orellano & Sperling, 2007) 20% of air resistance generated by regional train is contributed by protruding objects. Therefore, assuming 15 000 N air resistance is generated by others and 5000 N generated by protruding objects. The contribution of ET425M protruding air conditioning design to the total 5000 N is determined with the obtained drag force from the simulation. The remaining drag force of protruding objects remained as constant. The drag force generated by air

conditioning units act as manipulative coefficient. The governing equations are as follows:

Total drag force of remaining protruding objects=5000-B

Where,
B: Drag force of protruding air conditioning unit.

Total air resistance= 15000 + B + C

Where,

B: Drag force of air conditioning unit
C: Drag force of remaining protruding objects

The tractive effort of ET425M at 160 Km/h is 30000 N plus total air resistance. The differential factor between tractive effort with original air conditioning design and new improved air conditioning design is established.

The differential factor is used with actual power consumption of ET425M which are 279KWh (ERL, personal communication, 16 June 2019) and the difference in KWh is calculated in current commercial electric tariff of E2 by Tenaga Nasional Bhd which as of July 2019, RM0.337/Kwh to reflect the monetary difference. The difference in power consumption is calculated to act as basis to understand the relationship between air resistance and power consumption.

# 4. RESULTS & DISCUSSION

## 4.1. Drag Force & Drag Coefficient

The total drag forces which consist of both drag fore due to pressure force and due to viscous force and total drag coefficient due to pressure force and viscous force for original design, model A, model B and model c is tabulated as below tables. The original design and all suggested new design of model A, model B and model C is simulated with inlet velocity of 160Km/h, 140Km/h, 120Km/h and 100 Km/h.

Table 4.1: Drag force & drag coefficient of original air conditioning unit design

| **Speed (Km/h)** | **Pressure (N)** | **Viscous (N)** | **Total (N)** | **Cd** |
|---|---|---|---|---|
| 160 | 2688 | 1166 | 3854 | 0.56 |
| 140 | 2061 | 910 | 2971 | 0.57 |
| 120 | 1517 | 684 | 2201 | 0.57 |
| 100 | 1055 | 488 | 1543 | 0.58 |

Table 4.2: Drag force & drag coefficient of model A

| **Speed (Km/h)** | **Pressure (N)** | **Viscous (N)** | **Total (N)** | **Cd** |
|---|---|---|---|---|
| 160 | 2047 | 1140 | 3187 | 0.46 |
| 140 | 1569 | 890 | 2460 | 0.47 |
| 120 | 1155 | 670 | 1825 | 0.47 |
| 100 | 804 | 478 | 1282 | 0.48 |

Table 4.3: Drag force & drag coefficient of model B

| **Speed (Km/h)** | **Pressure (N)** | **Viscous (N)** | **Total (N)** | **Cd** |
|---|---|---|---|---|
| 160 | 1859 | 1132 | 2991 | 0.44 |
| 140 | 1426 | 884 | 2310 | 0.44 |
| 120 | 1049 | 665 | 1714 | 0.44 |
| 100 | 729 | 474 | 1203 | 0.44 |

Table 4.4: Drag force & drag coefficient of model C

| Speed (Km/h) | Pressure (N) | Viscous (N) | Total (N) | Cd |
|---|---|---|---|---|
| 160 | 1696 | 1127 | 2823 | 0.41 |
| 140 | 1302 | 882 | 2184 | 0.41 |
| 120 | 959 | 662 | 1621 | 0.41 |
| 100 | 668 | 474 | 1142 | 0.41 |

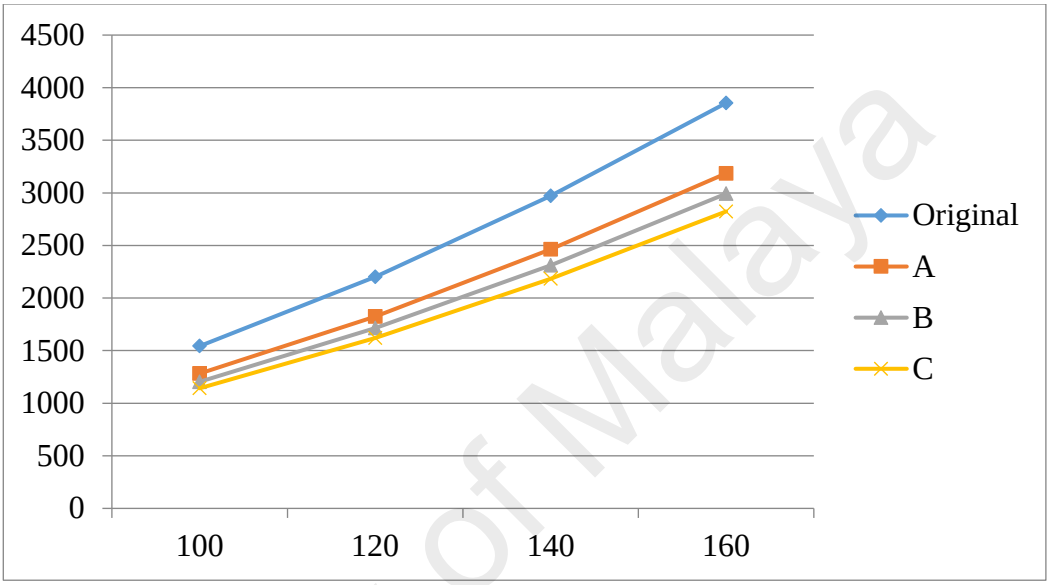


Figure 4.1: Total drag force (N) versus train velocity (Km/h) graph

As showed by figure 4.1, the total drag force acted on original air conditioning design of ET425M showed trend of decreasing with introduction of air deflector with various angles. The difference between original design and model A which air conditioning unit designed with air deflector angle of 40 degree at each unit showed reduction of 18% with train velocity of 160Km/h. With subsequent train velocity, the reduction of drag force showed consistent 18% reduction. The difference between original design and model B which is air conditioning unit designed with air deflector of 30 degrees at each unit showed reduction of 23% with train velocity of 160Km/h. With subsequent train velocity, the reduction of drag force showed consistent 23% reduction. The difference between original design and model C which is air conditioning unit designed with air deflector of

20 degrees at each unit showed reduction of 27% with train velocity of 160Km/h. With subsequent train velocity, the reduction of drag force showed consistent 27% reduction. The introduction of air deflector with 40 degree managed to reduce 18% of drag force while varying the deflection angle showed reduction of maximum 9% from model A. The result obtained is consistent with research conducted by Ramesh et al (2017) which is by optimizing air deflector angle managed to reduce initial drag by maximum 17.6% as demonstrated in the research.

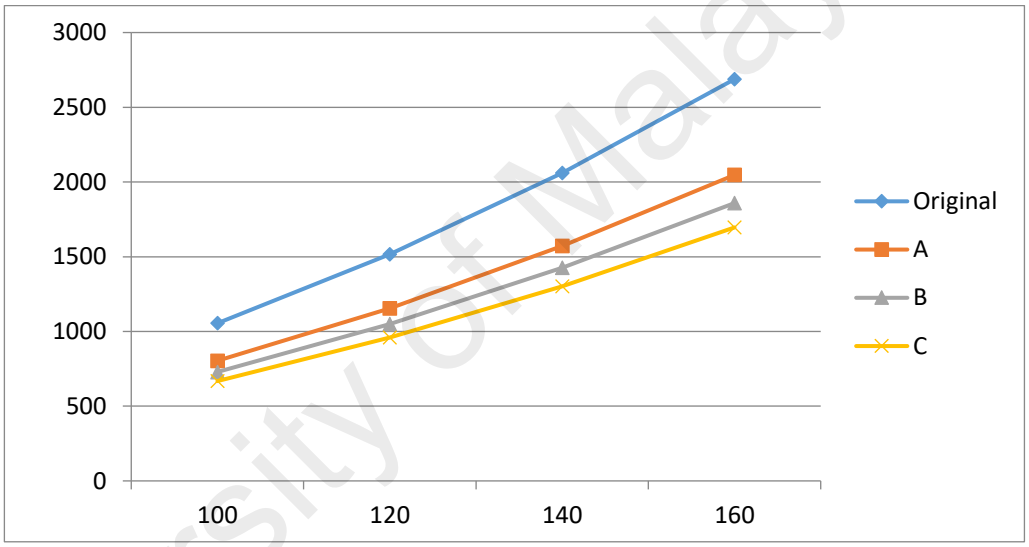


Figure 4.2: Drag force due to pressure (N) versus train velocity (Km/h) graph

As showed in figure 4.2, drag force to pressure for each model showed consistent with angle deflector design. With introduction of air deflector with angle of 40 degree showed reduction of 24% with train velocity of 160Km/h. Reduction of 31% showed with introduction of air deflector with angle of 30 degree. Reduction of 37% showed with introduction of air deflector with angle of 20%. Tremendous 24% reduction achieved by introducing air deflector with angle of 40% while varying the air deflector showed reduction of max 13%.

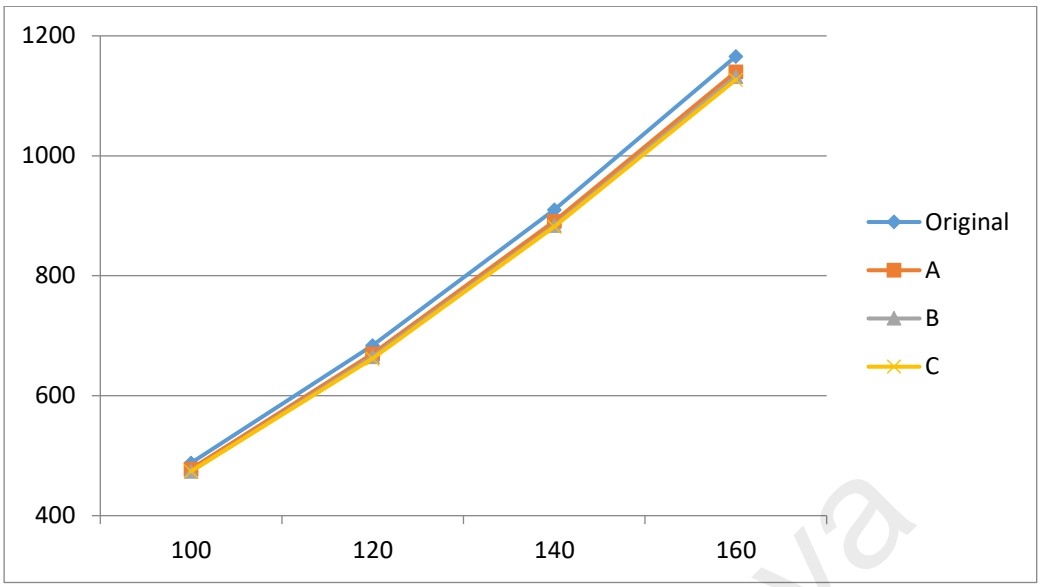


Figure 4.3: Drag force due to viscous (N) versus train velocity (Km/h) graph

As shows in figure 4.3, drag force to viscous showed insignificant difference with introduction of air deflector with any angle.

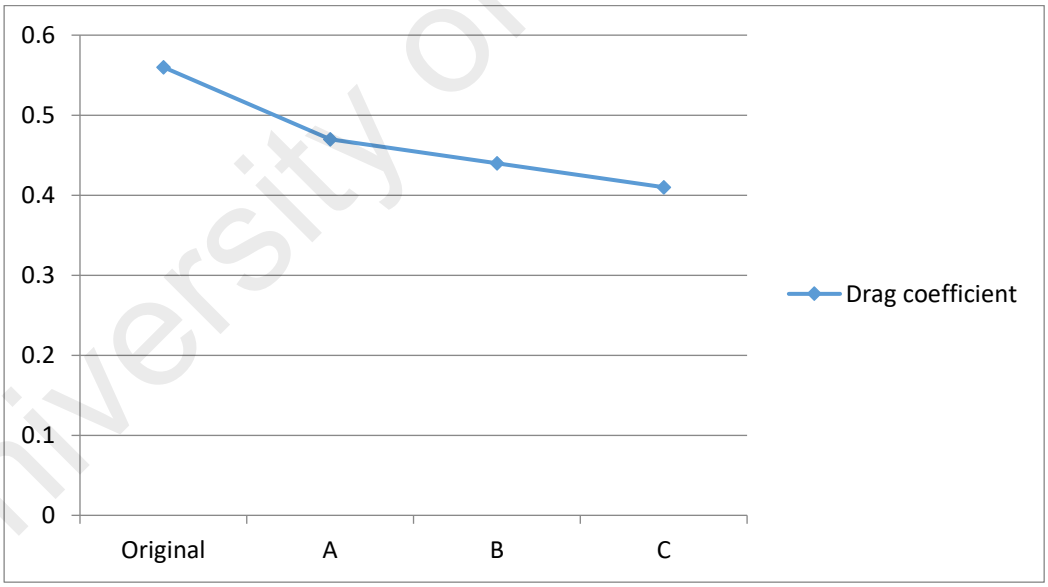


Figure 4.4: Drag coefficient versus air conditioning unit design graph

As showed in figure 4.4, initial drag coefficient of air conditioning unit showed significant reduction of 18% with introduction of air deflector angle of 40 degree. However, the trend of reduction in drag coefficient showed steady decrease pattern with reduction between A, B and C varies between 5% to 11%

4.2. Max Pressure

The max pressure exerted by original design, model A, model B and model C when simulated with inlet velocity of 160Km/h,140Km/h,120Km/h and 100Km/h is tabulated as below table.

Table 4.5: Relationship between air deflector angle and max pressure (Pa)

| **Speed (Km/h)** | **Max pressure(Pa) Model Original** | **Max pressure(Pa) Model A** | **Max pressure(Pa) Model B** | **Max pressure(Pa) Model C** |
|---|---|---|---|---|
| 160 | 1389 | 1061 | 869 | 760 |
| 140 | 1067 | 815 | 668 | 585 |
| 120 | 787 | 602 | 494 | 433 |
| 100 | 549 | 420 | 345 | 308 |

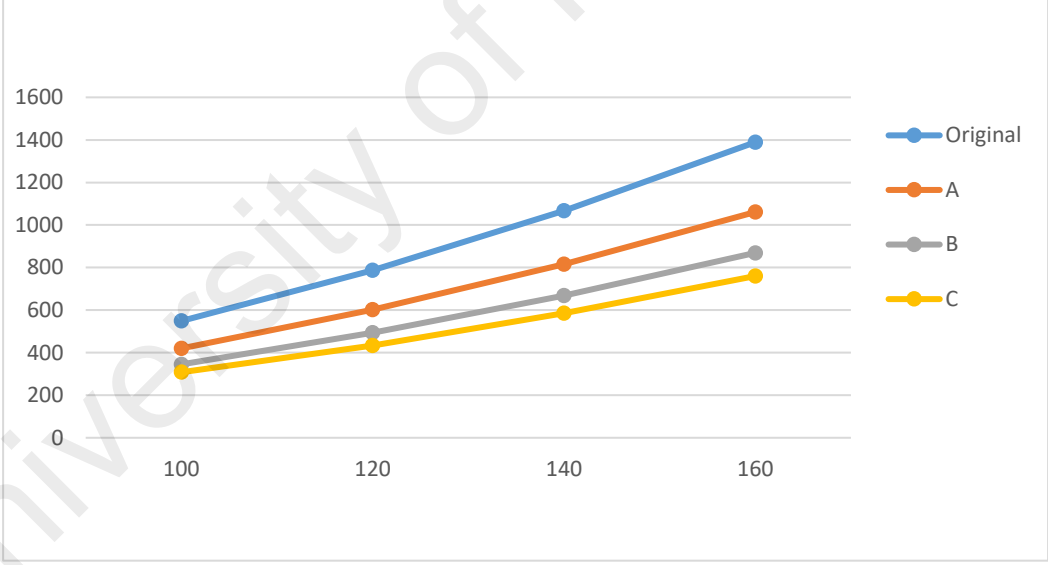


Figure 4.5: Max pressure (Pa) versus train velocity (Km/h) graph

As showed in figure 4.5, max pressure exerted by original design showed trend of increase as pressure build at air conditioning unit due to air deflector is not in place. However, with introduction of air deflector, the max pressure registered a significant reduction of 24% at train velocity of 160Km/h.

This is due to the build-up pressure been eased off by air deflector and the stagnation points been mitigated.

With various manipulation of air deflector angle from 30 degree to 20 degree, the reduction in max pressure registered additional reduction of 14% to 22%.

4.3. Power Consumption

Table 4.6: Relationship between air conditioning units resistance (N) to tractive effort to establish the differential factor

| Model | Air-condition units resistance (N) | Protruding objects resistance (N) | Total motion resistance (N) | Tractive effort (N) | Differential factor |
|---|---|---|---|---|---|
| Original | 3854 | 5000 | 50000 | 50000 | - |
| C | 2823 | 3969 | 48969 | 48969 | 0.97 |

Table 4.7: Power consumption of ET425M new air conditioning unit design based on actual power consumption of 279 KWh.

| Model | Differential factor | Power consumption per trip in KWh | Power consumption cost per trip in RM |
|---|---|---|---|
| Original | 1 | 279 | 94 |
| C | 0.97 | 270 | 91 |

Table 4.8: Power consumption of original ET425M air conditioning unit design and with air conditioning unit design of model C.

| Model | Power consumption for one day (237 trips) in KWh | Power consumption for one month in KWh | Power consumption for one year in KWh |
|---|---|---|---|
| Original | 66,123 | 2,049,813 | 24,597,756 |
| C | 64,139 | 1,988,319 | 23,859,823 |

Table 4.9: Power consumption cost of original ET425M air conditioning unit design and with air conditioning unit design of model C.

| Model | Power consumption per day (237 trips) in RM | Power consumption per month in RM | Power consumption per year in RM |
|---|---|---|---|
| Original | 22,278 | 690,618 | 8,287,416 |
| C | 21,609 | 669,899 | 8,038,794 |

Table 4.10: Power consumption cost difference of original ET425M air conditioning unit design and with air conditioning unit design of model C.

| Model | Difference of power consumption for 1 year in RM | Difference of power consumption for 20 years in RM | Difference of power consumption for 30 years in RM |
|---|---|---|---|
| Original | 0 | 0 | 0 |
| C | 248,622 | 4,972,450 | 7,458,674 |

A 3% reduction is established in power consumption using approximation approach with various assumptions to establish relationship between reduction in air resistance and power consumption. The figures do not reflect actual saving as the method used is not proven method relating reduction of motion resistance with power consumption. However, it gave an understanding that even a slight reduction in power consumption reflects a significant amount in monetary aspect in a long run.

Table 4.11: Relationship between approximate reductions in power consumption with cost

| Approximate reduction | Difference of power consumption cost for 10 years in RM | Difference of power consumption cost for 20 years in RM | Difference of power consumption cost for 30 years in RM |
|---|---|---|---|
| 1% | 828,741 | 1,657,483 | 2,486,255 |
| 2% | 1,657,483 | 3,314,966 | 4,972,450 |
| 3% | 2,486,225 | 4,972,450 | 7,458,674 |

As showed in table 4.11, even with approximate reduction of 1% power consumption, it generated a significant saving in power consumption cost in long term.

# 5. CONCLUSION

As the results showed, with just introduction of air deflector to the design of air a very significant reduction in aerodynamic resistance. With reduction of aerodynamic shall be reduction in traction effort in basic law of motion. The reduced traction effort leads to lead traction power need to be produce by the train traction motor, hence leads to reduce of power consumption. Reduced power consumption leads to reduced power consumption cost. The actual reduction of power consumption by reduction of aerodynamic resistance not been established in the research project. However, it set a basis and understanding the ignored additional power consumption due to ignored additional aerodynamic resistance leads to huge amount of wastage in monetary aspect. As ET425M is designed to be in operation for 30 years, an additional drag resistance should be mitigated during design stage as it will be bringing a significant amount in monetary perspective.

Incorporating air deflector design to air conditioning unit is expected not produce any huge amount in cost as it just may require a simple version of air spoiler with light material. The potential reduction in drag resistance by optimization of the design must take in account with design that expected with long operational expectancy as small percentage reduction in energy consumed contributed a huge amount in long term. With realize the potential of reduction drag resistance to saving in energy consumption cost will leads to greater effort in optimizing drag reduction in any design that known incurred additional small drag resistance. A model to predict reduction in drag resistance with power consumption especially in electric powered train should be developed in the future to understand the potential of optimizing drag reduction design.

## 6. REFERENCES


Alexander Orellano & Stefan Sperling (2007). Aerodynamic improvements and associated energy demand reduction of trains.

Coals Newcastle (2017). The application of Davis formula to set train resistance in open rails.

Cihan Bagindirli (2017). The experimental investigation of the effects of spoiler design on aerodynamic drag coefficient on truck trailer combination.

Heinz Heisler (2002). Vehicle body aerodynamic.

Harun Chowdhury, Hazim Moria, AbdulKadir Ali, Iftekhar Khan, Firoz Alam & Simon Watkins (2013). A study on aerodynamic drag of a semi-trailer truck.

James C. Paul, Richard W. Johnson & Robert G. Yates (2007). Application of CFD to rail car and locomotive aerodynamics.

Jyh Cheng Jong & En Fo Ghang (2005). Models for estimating energy consumption of electric train.

K. Gemba (2007). Shape effects on drag

Monroe Corner (2017). NASA Armstrong fact sheet: Aerodynamic truck studies.

Ramesh DK, Rajesha R, Snehahree KB, Shashrna A Bhat, Marogna NR (2017). Aerodynamic analysis and optimization of wind deflector in a commercial land transport vehicle.

Seyyed Khandani (2005). Engineering design process.

Shane Maxemow (2009). The effect of drag forces.

Siemens (2000). ET425M technical description produced by Siemens on year 2000 for Express Rail Link.

Tae-Hwan Joung, Hyeung-Sik Choi, Sang-Wi Jung, Karl Sammut, Fung Po He (2014). Verification of CFD analysis methods for predicting the drag force and thrust power of an underwater disk robot.

.

\

## APPENDIX A: ET425M air conditioning unit design drawing

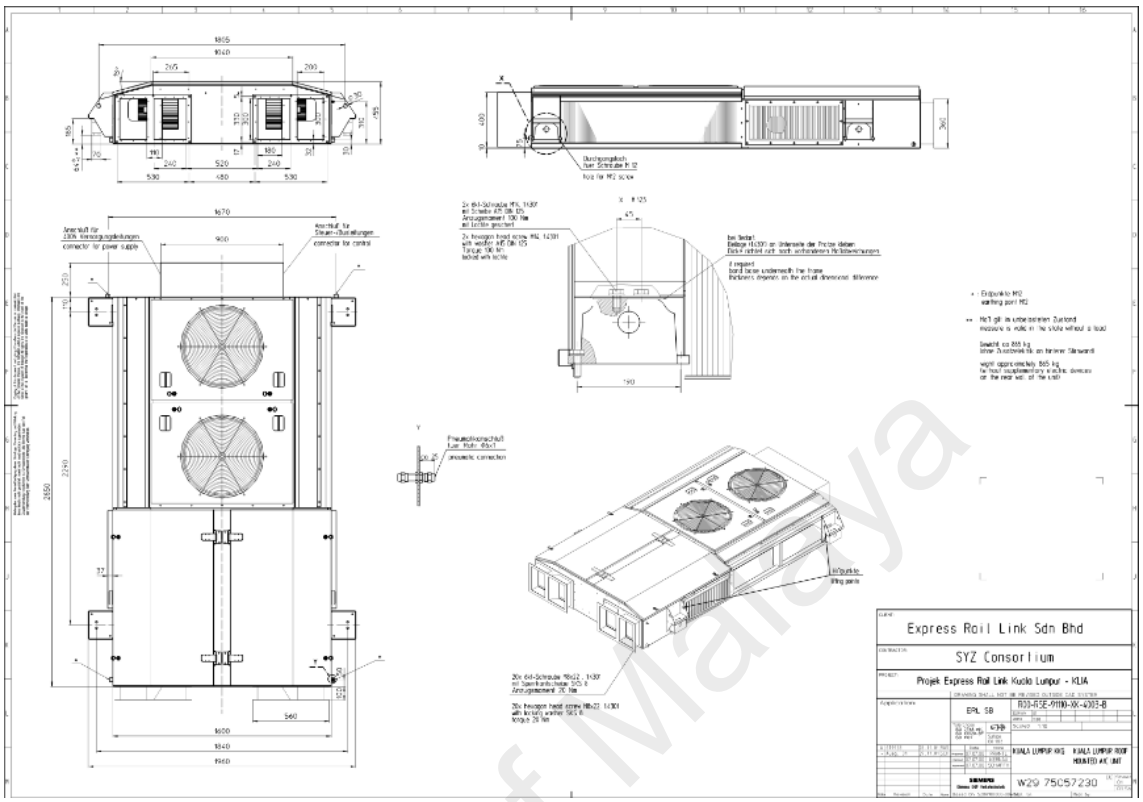

## APPENDIX B: Mesh details for original air conditioning unit design

Details of "Mesh"

| | |
|---|---|
| **Display** | |
| Display Style | Use Geometry Setting |
| **Defaults** | |
| Physics Preference | CFD |
| Solver Preference | Fluent |
| Element Order | Program Controlled |
| Element Size | 0.5 m |
| Export Format | Standard |
| Export Preview Surface Mesh | No |
| **Sizing** | |
| Use Adaptive Sizing | No |
| Growth Rate | Default (1.2) |
| Max Size | Default (1.0 m) |
| Mesh Defeaturing | Yes |
| Defeature Size | Default (2.5e-003 m) |
| Capture Curvature | Yes |
| Curvature Min Size | Default (5.e-003 m) |
| Curvature Normal Angle | Default (18.0°) |
| Capture Proximity | No |
| Bounding Box Diagonal | 66.257 m |
| Average Surface Area | 45.789 $m^2$ |
| Minimum Edge Length | 1.e-002 m |
| **Quality** | |
| **Inflation** | |
| **Assembly Meshing** | |
| **Advanced** | |
| **Statistics** | |
| Nodes | 94019 |
| Elements | 60963 |

## APPENDIX C: Mesh details for model A

Details of "Mesh"

| | |
|---|---|
| **Display** | |
| Display Style | Use Geometry Setting |
| **Defaults** | |
| Physics Preference | CFD |
| Solver Preference | Fluent |
| Element Order | Program Controlled |
| Element Size | 0.5 m |
| Export Format | Standard |
| Export Preview Surface Mesh | No |
| **Sizing** | |
| Use Adaptive Sizing | No |
| Growth Rate | Default (1.2) |
| Max Size | Default (1.0 m) |
| Mesh Defeaturing | Yes |
| Defeature Size | Default (2.5e-003 m) |
| Capture Curvature | Yes |
| Curvature Min Size | Default (5.e-003 m) |
| Curvature Normal Angle | Default (18.0°) |
| Capture Proximity | No |
| Bounding Box Diagonal | 66.257 m |
| Average Surface Area | 40.677 $m^2$ |
| Minimum Edge Length | 7.5942e-003 m |
| **Quality** | |
| **Inflation** | |
| **Assembly Meshing** | |
| **Advanced** | |
| **Statistics** | |
| Nodes | 94335 |
| Elements | 61134 |

## APPENDIX D: Mesh details for model B

Details of "Mesh"

| | |
|---|---|
| **Display** | |
| Display Style | Use Geometry Setting |
| **Defaults** | |
| Physics Preference | CFD |
| Solver Preference | Fluent |
| Element Order | Program Controlled |
| Element Size | 0.5 m |
| Export Format | Standard |
| Export Preview Surface Mesh | No |
| **Sizing** | |
| Use Adaptive Sizing | No |
| Growth Rate | Default (1.2) |
| Max Size | Default (1.0 m) |
| Mesh Defeaturing | Yes |
| Defeature Size | Default (2.5e-003 m) |
| Capture Curvature | Yes |
| Curvature Min Size | Default (5.e-003 m) |
| Curvature Normal Angle | Default (18.0°) |
| Capture Proximity | No |
| Bounding Box Diagonal | 66.257 m |
| Average Surface Area | 40.682 $m^2$ |
| Minimum Edge Length | 5.2253e-003 m |
| **Quality** | |
| **Inflation** | |
| **Assembly Meshing** | |
| **Advanced** | |
| **Statistics** | |
| Nodes | 94125 |
| Elements | 61043 |

## APPENDIX E: Mesh details for model C

Details of "Mesh"

| | |
|---|---|
| **Display** | |
| Display Style | Use Geometry Setting |
| **Defaults** | |
| Physics Preference | CFD |
| Solver Preference | Fluent |
| Element Order | Program Controlled |
| Element Size | 0.5 m |
| Export Format | Standard |
| Export Preview Surface Mesh | No |
| **Sizing** | |
| Use Adaptive Sizing | No |
| Growth Rate | Default (1.2) |
| Max Size | Default (1.0 m) |
| Mesh Defeaturing | Yes |
| Defeature Size | Default (2.5e-003 m) |
| Capture Curvature | Yes |
| Curvature Min Size | Default (5.e-003 m) |
| Curvature Normal Angle | Default (18.0°) |
| Capture Proximity | No |
| Bounding Box Diagonal | 66.257 m |
| Average Surface Area | 40.7 $m^2$ |
| Minimum Edge Length | 3.2941e-003 m |
| **Quality** | |
| **Inflation** | |
| **Assembly Meshing** | |
| **Advanced** | |
| **Statistics** | |
| Nodes | 94082 |
| Elements | 60981 |

**APPENDIX F: Residual Scales drag coefficient & drag force for original design at 160 Km/h**

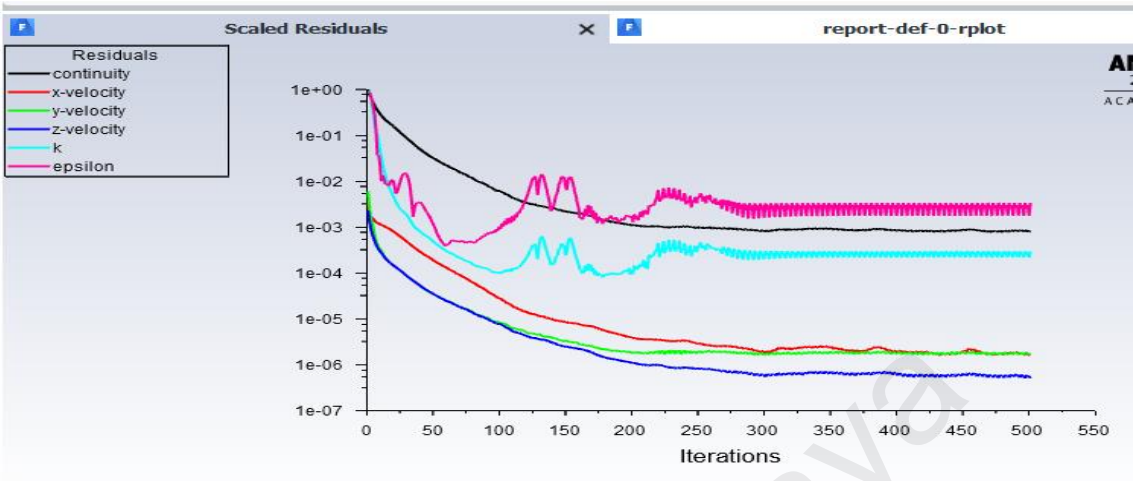


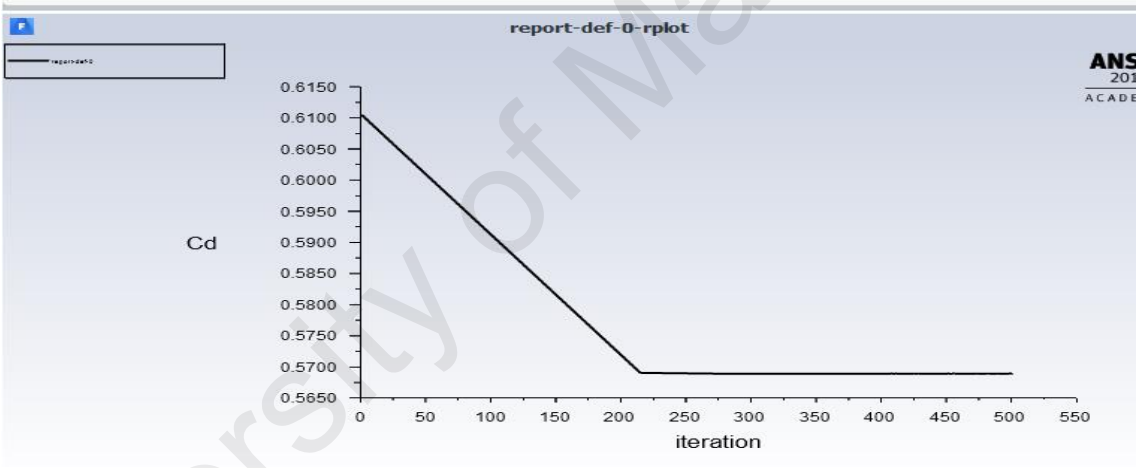


Forces - Direction Vector (-1 0 0)

| | Forces (n) | | | Coefficients | | |
|---|---|---|---|---|---|---|
| Zone | Pressure | Viscous | Total | Pressure | Viscous | Total |
| roof | 2688.5972 | 1166.0632 | 3854.6604 | 0.39682219 | 0.17210453 | 0.56892672 |
| Net | 2688.5972 | 1166.0632 | 3854.6604 | 0.39682219 | 0.17210453 | 0.56892672 |

## APPENDIX G: Residual Scales drag coefficient & drag force for original design at 140 Km/h

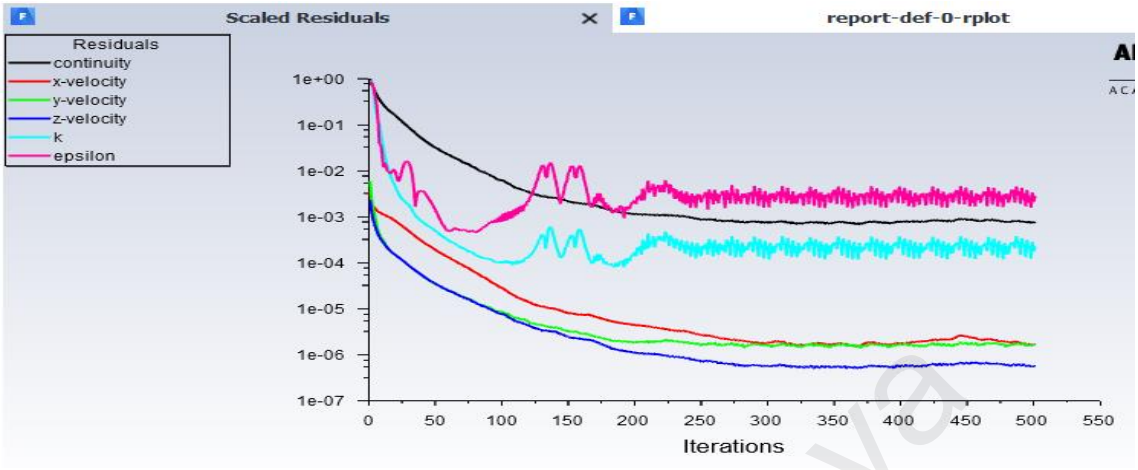


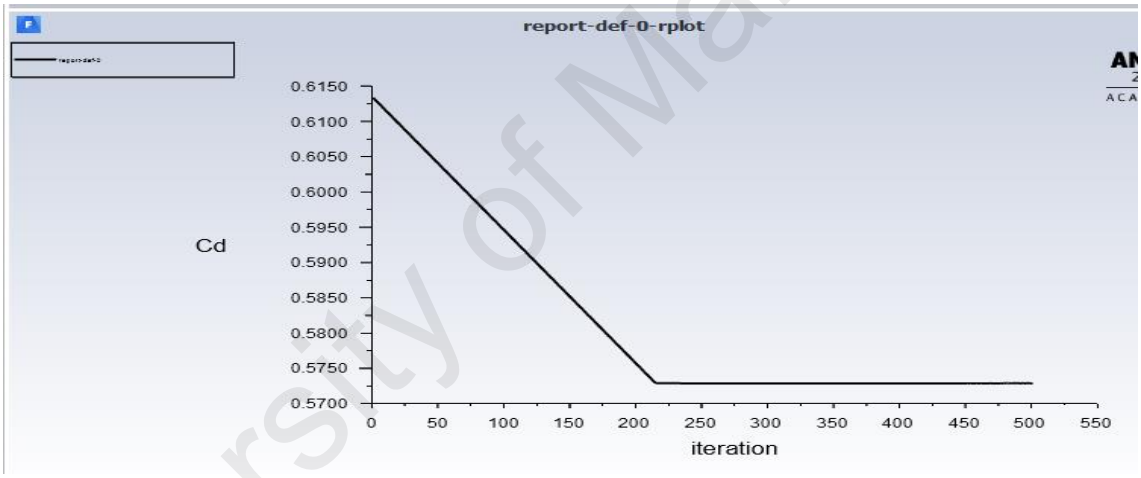


```
Forces - Direction Vector (-1 0 0)
                         Forces (n)                                    Coefficients
Zone                     Pressure        Viscous         Total         Pressure        Viscous         Total
roof                     2061.5422       910.26099       2971.8032     0.39741693      0.17547694      0.57289387
------------------------ --------------- --------------- ------------- --------------- --------------- ---------------
Net                      2061.5422       910.26099       2971.8032     0.39741693      0.17547694      0.57289387
```

## APPENDIX H: Residual Scales drag coefficient & drag force for original design at 120 Km/h

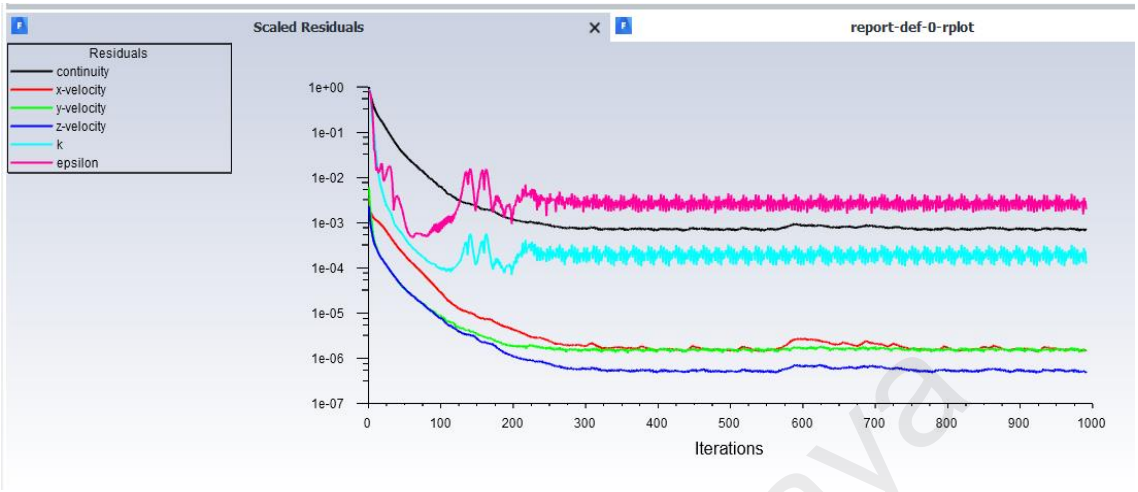


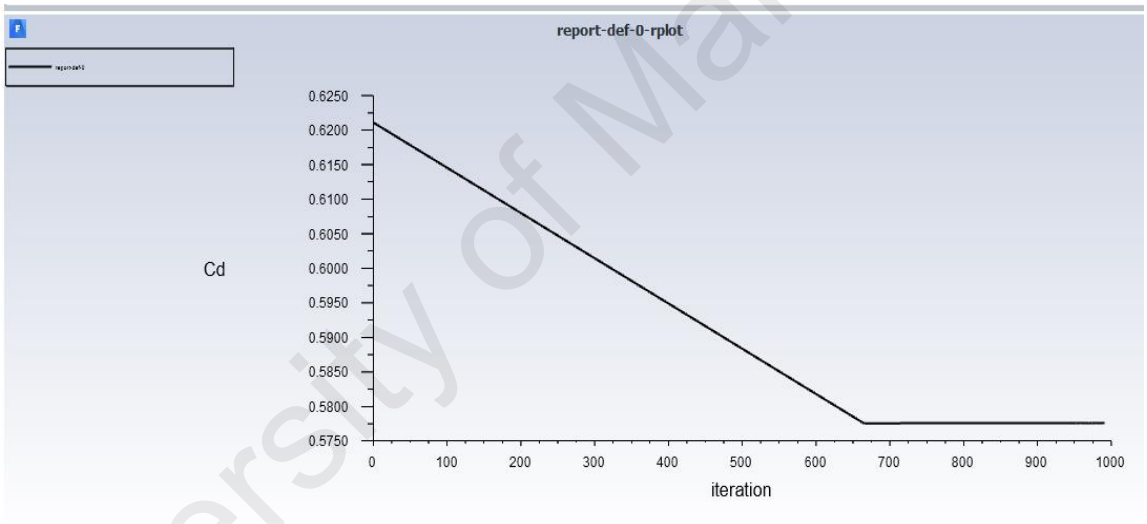


```
Forces - Direction Vector (-1 0 0)
                         Forces (n)                                    Coefficients
Zone                     Pressure        Viscous         Total         Pressure        Viscous         Total
roof                     1517.2008       684.03705       2201.2379     0.39809874      0.17948467      0.57758341
------------------------ --------------- --------------- ------------- --------------- --------------- ---------------
Net                      1517.2008       684.03705       2201.2379     0.39809874      0.17948467      0.57758341
```

**APPENDIX I: Residual Scales drag coefficient & drag force for original design at 100 Km/h**

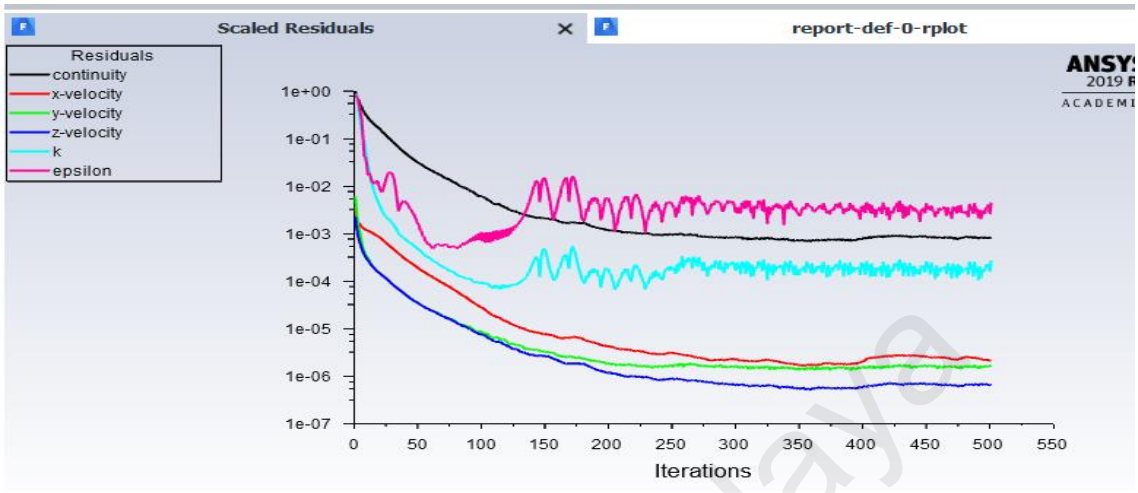


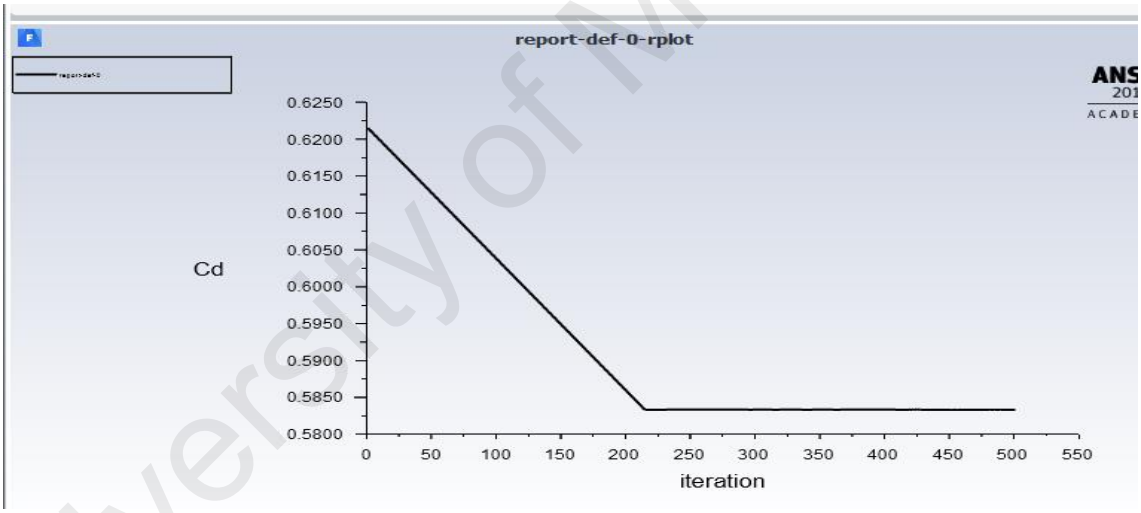


Forces - Direction Vector (-1 0 0)

| | Forces (n) | | | Coefficients | | |
|---|---|---|---|---|---|---|
| Zone | Pressure | Viscous | Total | Pressure | Viscous | Total |
| roof | 1055.7765 | 488.06958 | 1543.8461 | 0.39891668 | 0.18441318 | 0.58332985 |
| Net | 1055.7765 | 488.06958 | 1543.8461 | 0.39891668 | 0.18441318 | 0.58332985 |

## APPENDIX J: Residual Scales, drag coefficient & force for model A at 160 Km/h

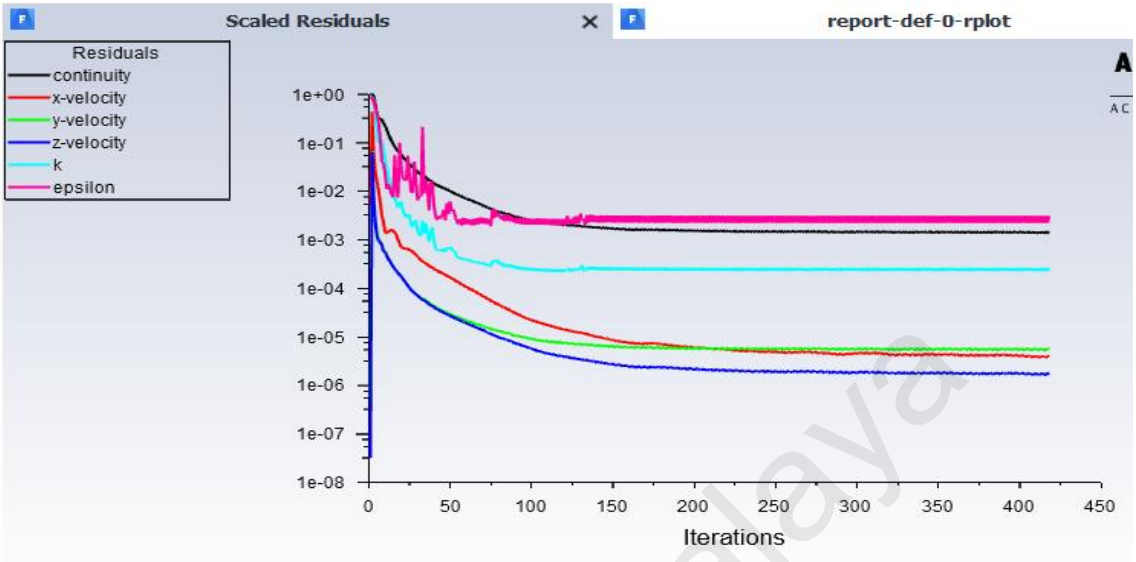


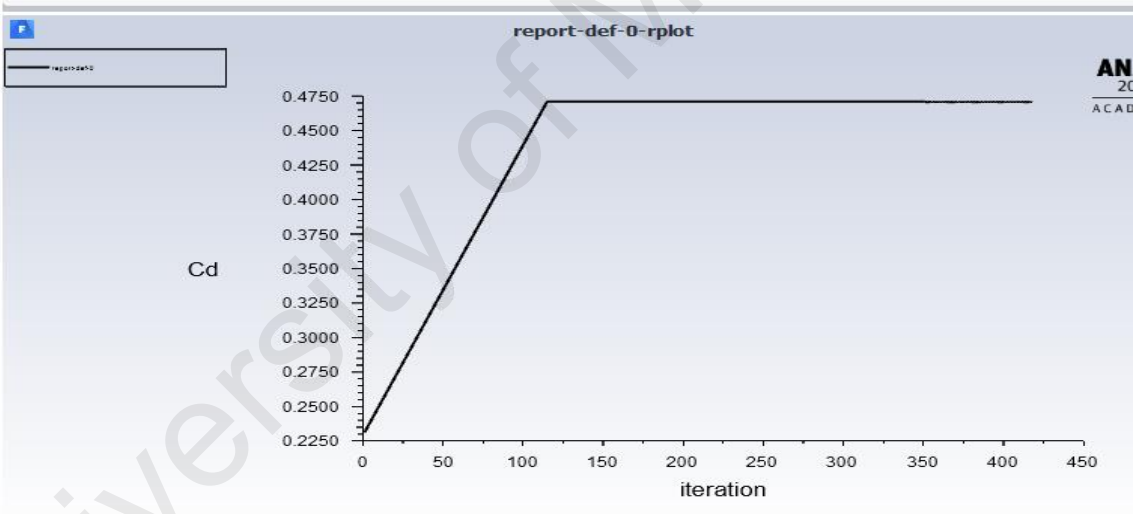


Forces - Direction Vector (-1 0 0)

| | Forces (n) | | | Coefficients | | |
|---|---|---|---|---|---|---|
| Zone | Pressure | Viscous | Total | Pressure | Viscous | Total |
| roof | 2047.3212 | 1140.6697 | 3187.9908 | 0.30217337 | 0.16835659 | 0.47052995 |
| Net | 2047.3212 | 1140.6697 | 3187.9908 | 0.30217337 | 0.16835659 | 0.47052995 |

## APPENDIX K: Residual Scales, drag coefficient & force for model A at 140 Km/h

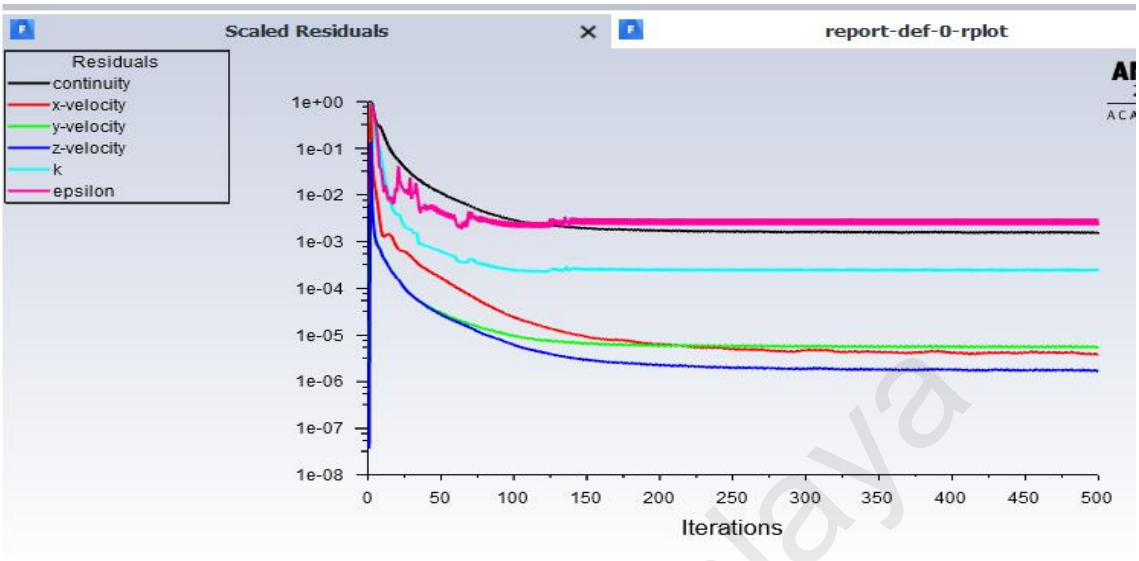


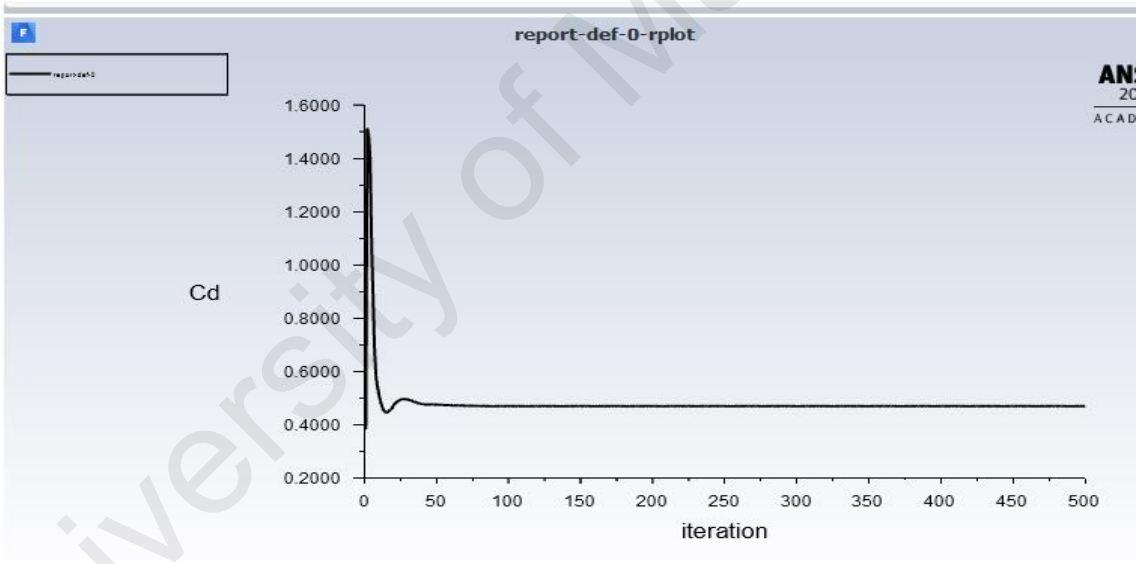


Console

```
Forces - Direction Vector (-1 0 0)
                          Forces (n)                                    Coefficients
Zone                      Pressure        Viscous         Total         Pressure        Viscous         Total
roof                      1569.3984       890.88184       2460.2803     0.30254316      0.1717411       0.47428426
------------------------- --------------- --------------- --------------- --------------- --------------- ---------------
Net                       1569.3984       890.88184       2460.2803     0.30254316      0.1717411       0.47428426
```

## APPENDIX L: Residual Scales, drag coefficient & force for model A at 120 Km/h

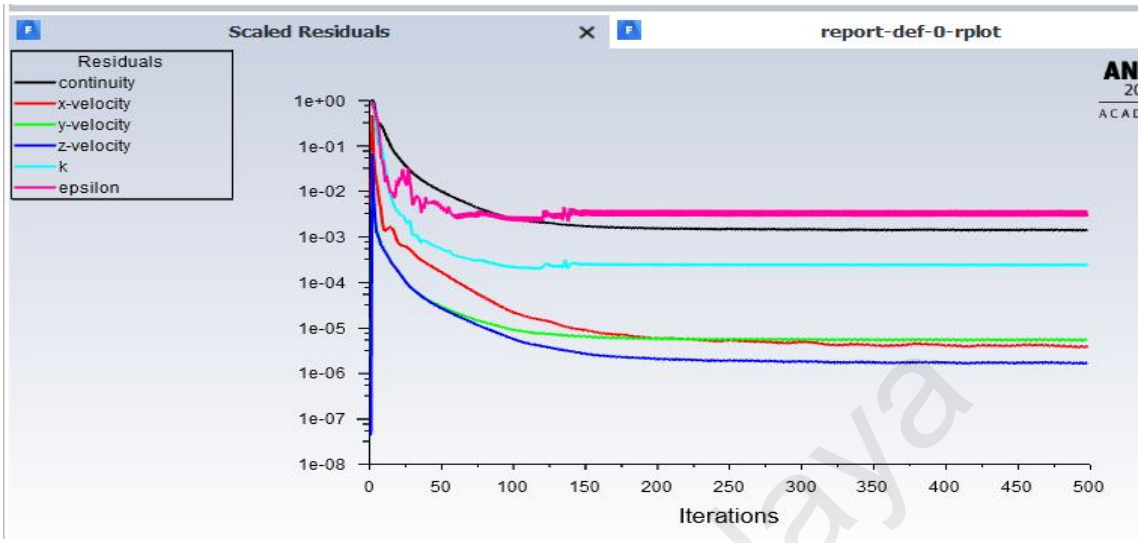


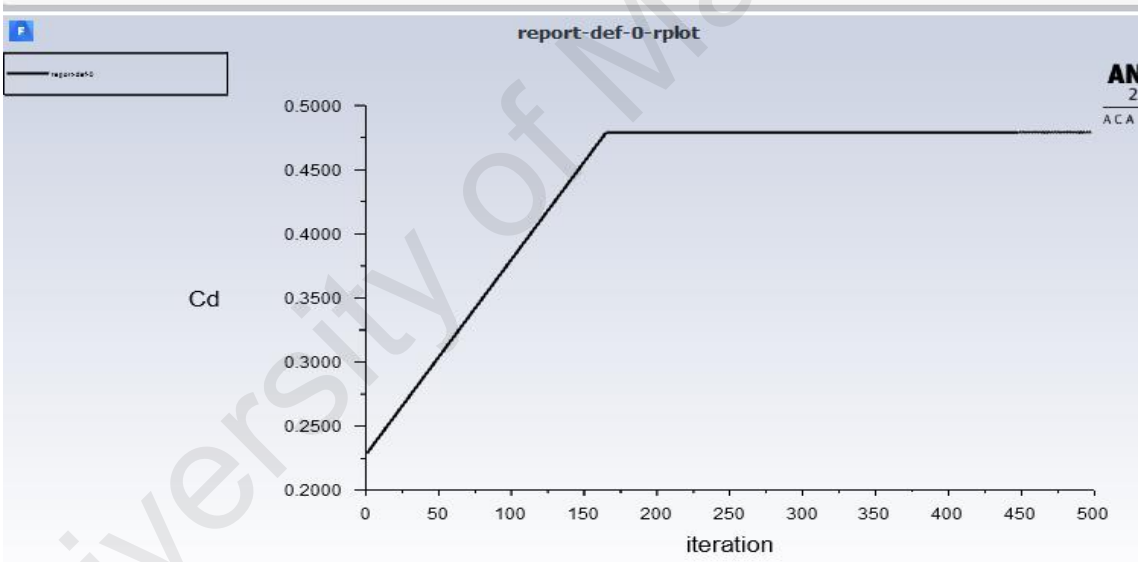


```
Forces - Direction Vector (-1 0 0)
                         Forces (n)                                    Coefficients
Zone                     Pressure        Viscous         Total         Pressure        Viscous         Total
roof                     1156.9156       670.21704       1827.1327     0.30356341      0.17585843      0.47942185
------------------------ --------------- --------------- ------------- --------------- --------------- ---------------
Net                      1156.9156       670.21704       1827.1327     0.30356341      0.17585843      0.47942185
```

## APPENDIX M: Residual Scales, drag coefficient & force for model A at 100 Km/h

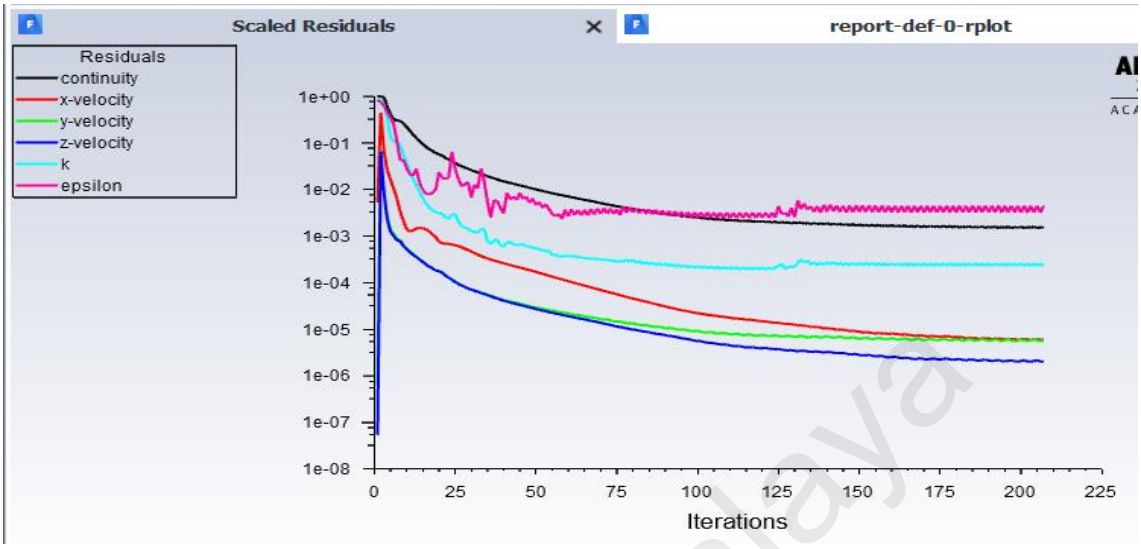


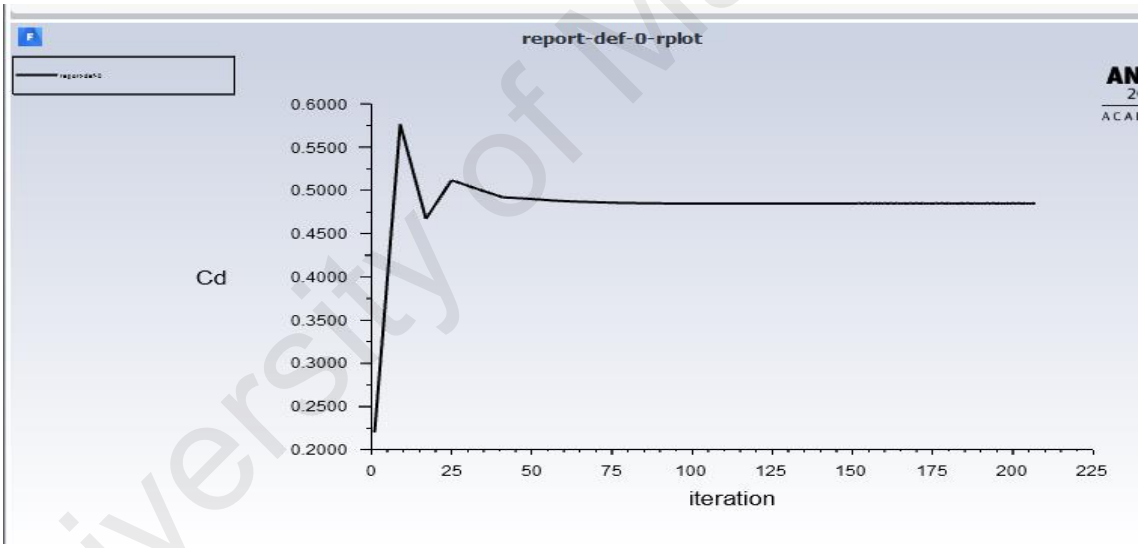


Forces - Direction Vector (-1 0 0)

| | Forces (n) | | | Coefficients | | |
|---|---|---|---|---|---|---|
| Zone | Pressure | Viscous | Total | Pressure | Viscous | Total |
| roof | 804.07227 | 478.5459 | 1282.6182 | 0.30381226 | 0.18081473 | 0.48462698 |
| Net | 804.07227 | 478.5459 | 1282.6182 | 0.30381226 | 0.18081473 | 0.48462698 |

## APPENDIX N: Residual Scales, drag coefficient & force for model B at 160 Km/h

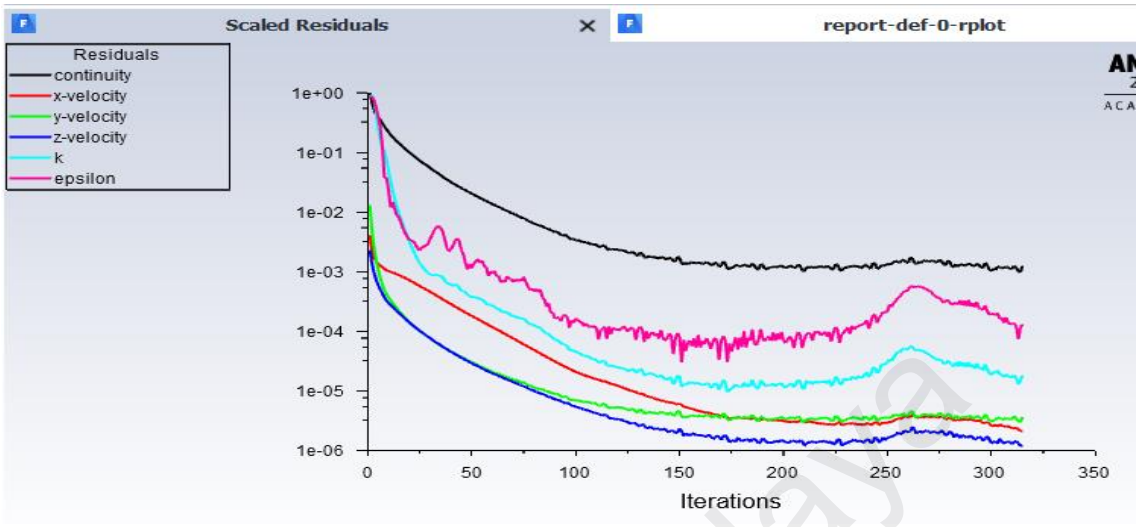


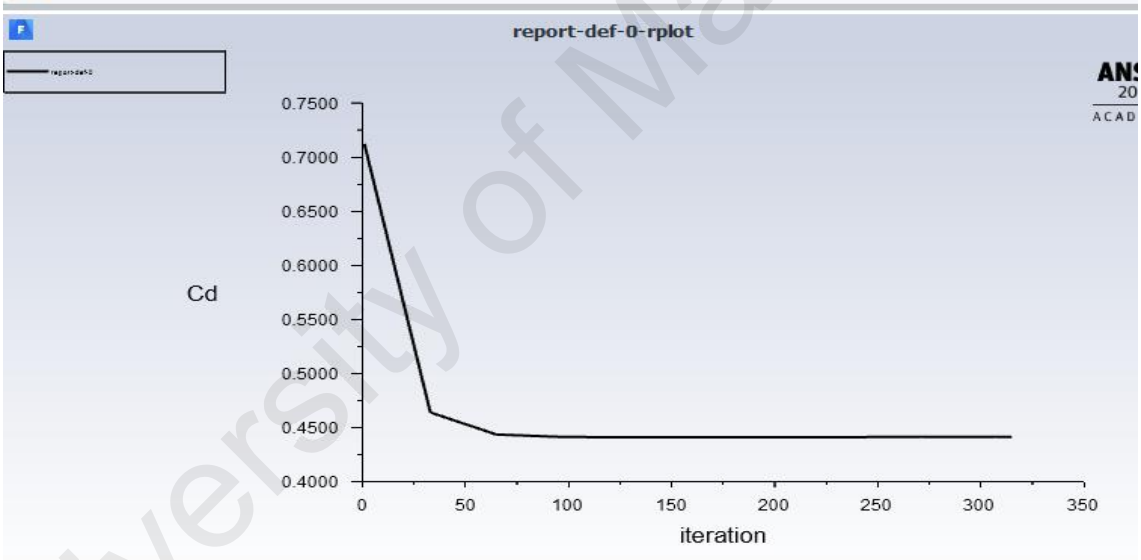


Forces - Direction Vector (-1 0 0)

| | Forces (n) | | | Coefficients | | |
|---|---|---|---|---|---|---|
| Zone | Pressure | Viscous | Total | Pressure | Viscous | Total |
| roof | 1859.896 | 1132.4967 | 2992.3927 | 0.27451044 | 0.1671503 | 0.44166074 |
| Net | 1859.896 | 1132.4967 | 2992.3927 | 0.27451044 | 0.1671503 | 0.44166074 |

## APPENDIX O: Residual Scales, drag coefficient & force for model B at 140 Km/h

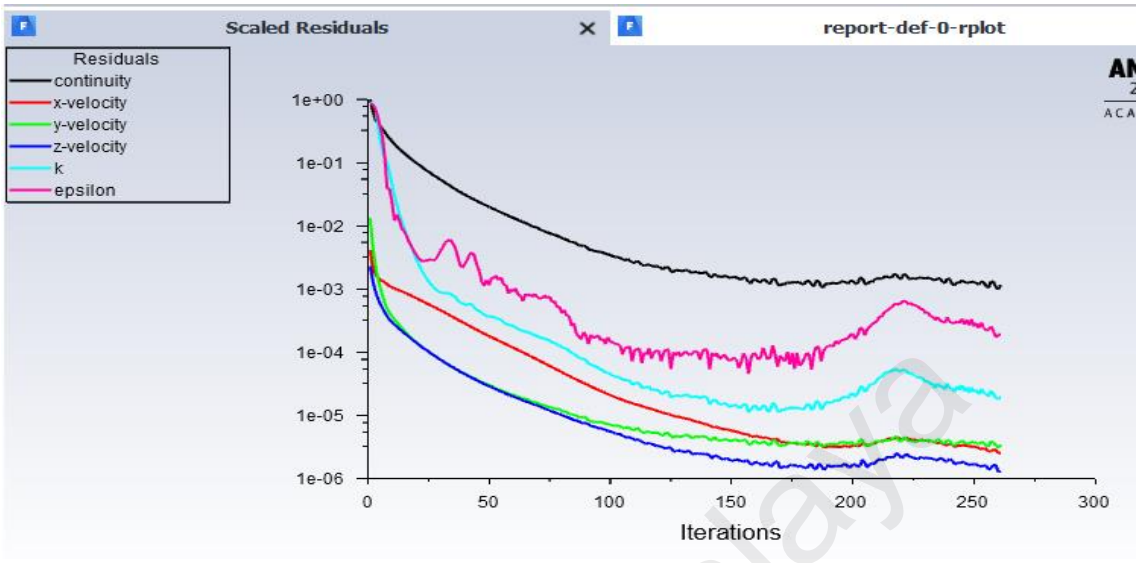


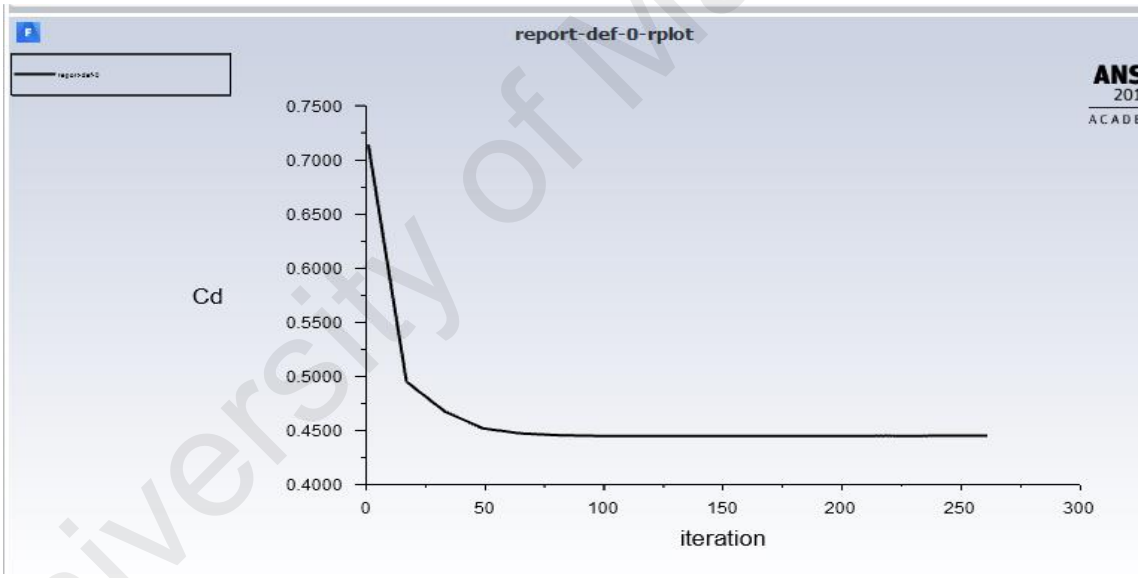


```
                          Forces (n)
Coefficients
Zone                      Pressure        Viscous         Total
Pressure         Viscous          Total
roof                      1426.2428       884.47675       2310.7195
0.27494612       0.17050635       0.44545246
------------------------- --------------- --------------- ---------------
```

## APPENDIX P: Residual Scales, drag coefficient & force for model B at 120 Km/h

```
Calculation complete.
```

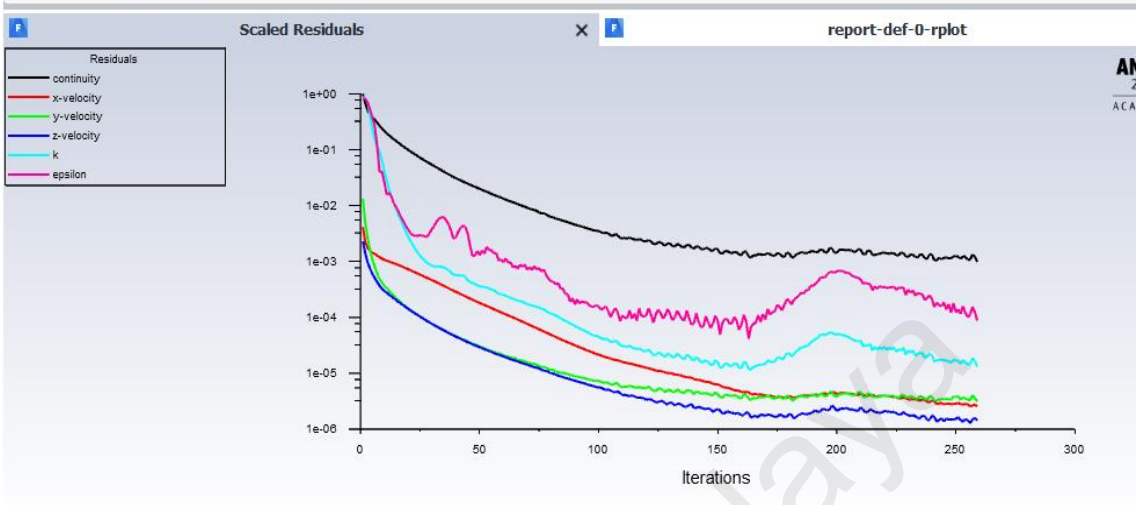


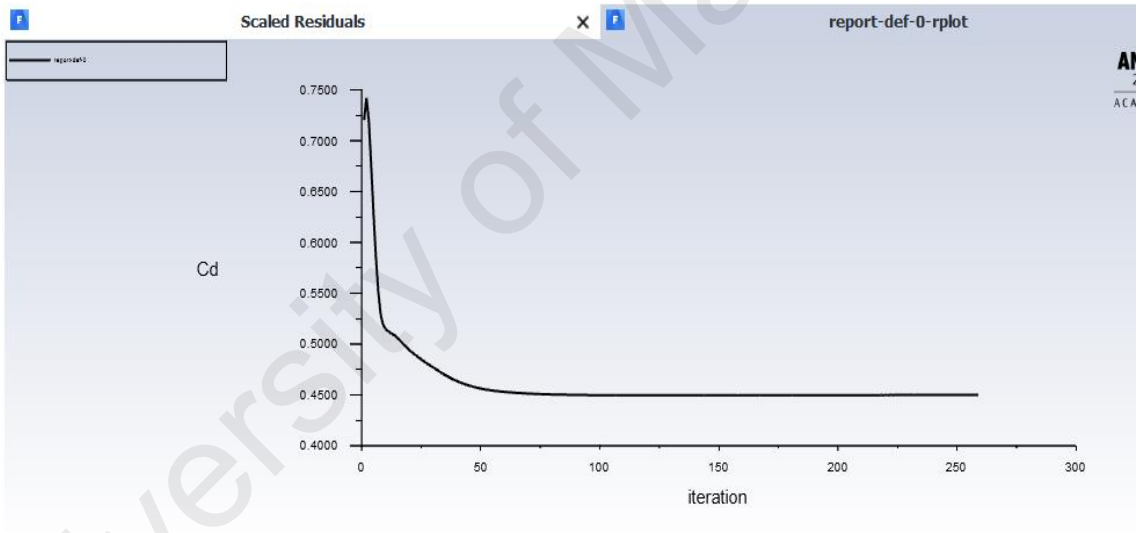


```
Forces - Direction Vector (-1 0 0)
                          Forces (n)                                    Coefficients
Zone                      Pressure        Viscous         Total         Pressure        Viscous         Total
roof                      1049.5394       665.11517       1714.6546     0.27538894      0.17451975      0.44990869
------------------------- --------------- --------------- ------------- --------------- --------------- ---------------
Net                       1049.5394       665.11517       1714.6546     0.27538894      0.17451975      0.44990869
```

# APPENDIX Q: Residual Scales, drag coefficient & force for model B at 100 Km/h

```
   149  1.2329e-03  5.1621e-06  3.9540e-06  2.1074e-06  1.5203e-05  9.0501e-05  4.5517e-01  0:03:00  348
   150  1.0244e-03  4.9510e-06  3.4808e-06  1.9721e-06  1.1928e-05  4.9386e-05  4.5516e-01  0:03:33  347
!  151 solution is converged
   151  9.9364e-04  4.5884e-06  3.3556e-06  1.6817e-06  1.2441e-05  7.6030e-05  4.5518e-01  0:02:50  346
Registering ReportDefFiles, ("C:\Users\nizac\Desktop\test_files\dp0\FFF-12\Fluent\report-def-0-rfile.out")
Writing data to C:\Users\nizac\Desktop\test_files\dp0\FFF-12\Fluent\FFF-12.ip ...
```

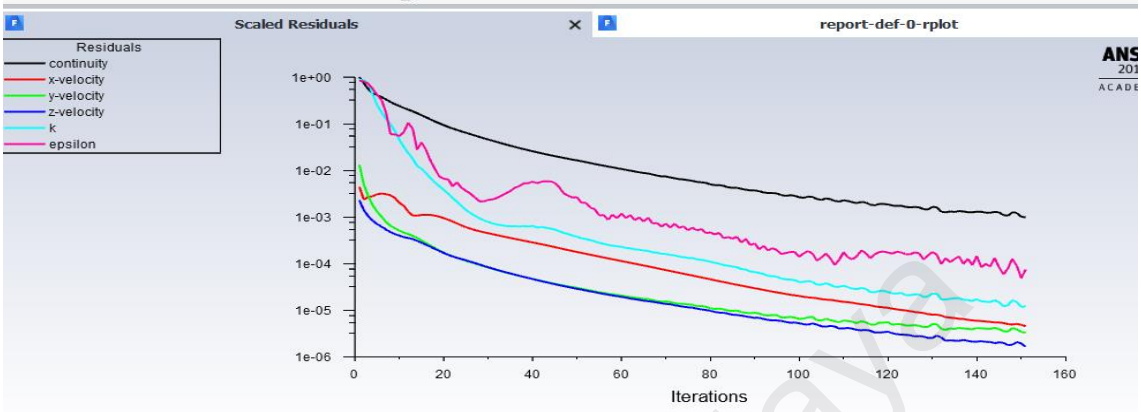


```
   149  1.2329e-03  5.1621e-06  3.9540e-06  2.1074e-06  1.5203e-05  9.0501e-05  4.5517e-01  0:03:00  348
   150  1.0244e-03  4.9510e-06  3.4808e-06  1.9721e-06  1.1928e-05  4.9386e-05  4.5516e-01  0:03:33  347
!  151 solution is converged
   151  9.9364e-04  4.5884e-06  3.3556e-06  1.6817e-06  1.2441e-05  7.6030e-05  4.5518e-01  0:02:50  346
Registering ReportDefFiles, ("C:\Users\nizac\Desktop\test_files\dp0\FFF-12\Fluent\report-def-0-rfile.out")
Writing data to C:\Users\nizac\Desktop\test_files\dp0\FFF-12\Fluent\FFF-12.ip ...
```

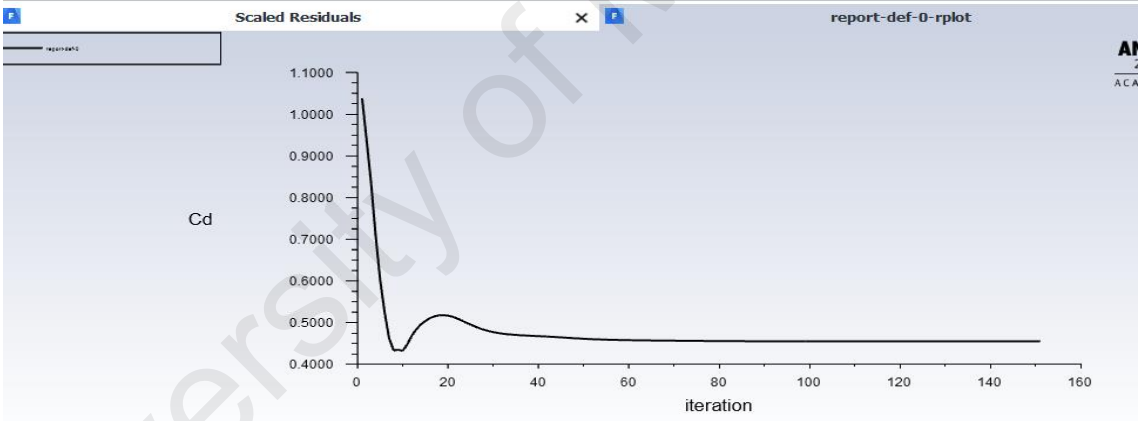


```
Forces - Direction Vector (-1 0 0)
                         Forces (n)                                    Coefficients
Zone                     Pressure        Viscous         Total         Pressure        Viscous         Total
roof                     729.69604       474.97485       1204.6709     0.2757098       0.17946544      0.45517524
------------------------ --------------- --------------- ------------- --------------- --------------- ---------------
Net                      729.69604       474.97485       1204.6709     0.2757098       0.17946544      0.45517524
```

## APPENDIX R: Residual Scales, drag coefficient & force for model C at 160 Km/h

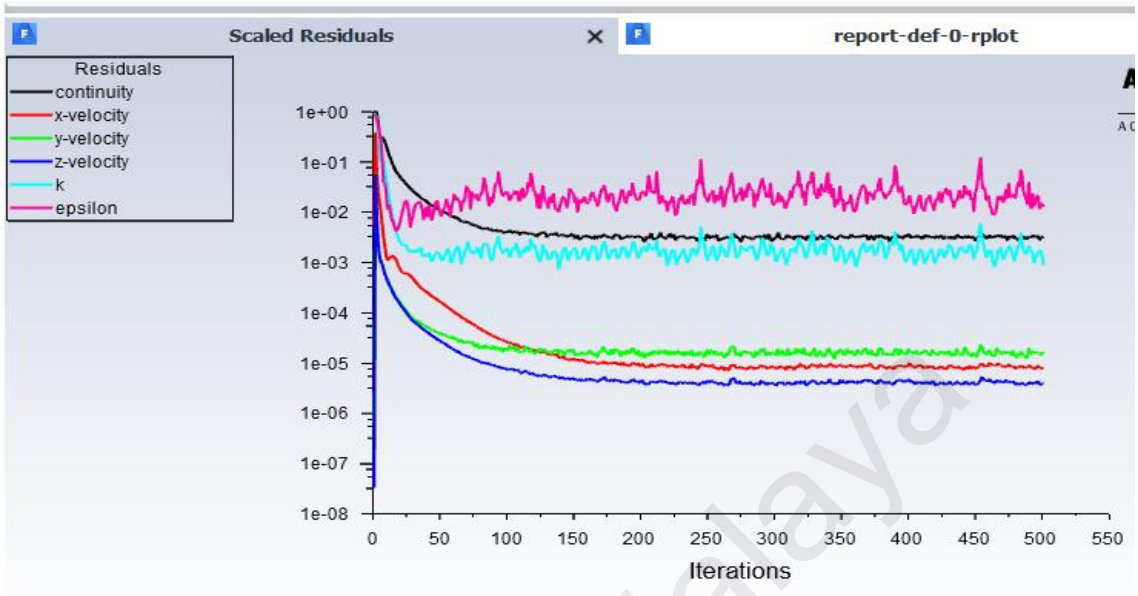


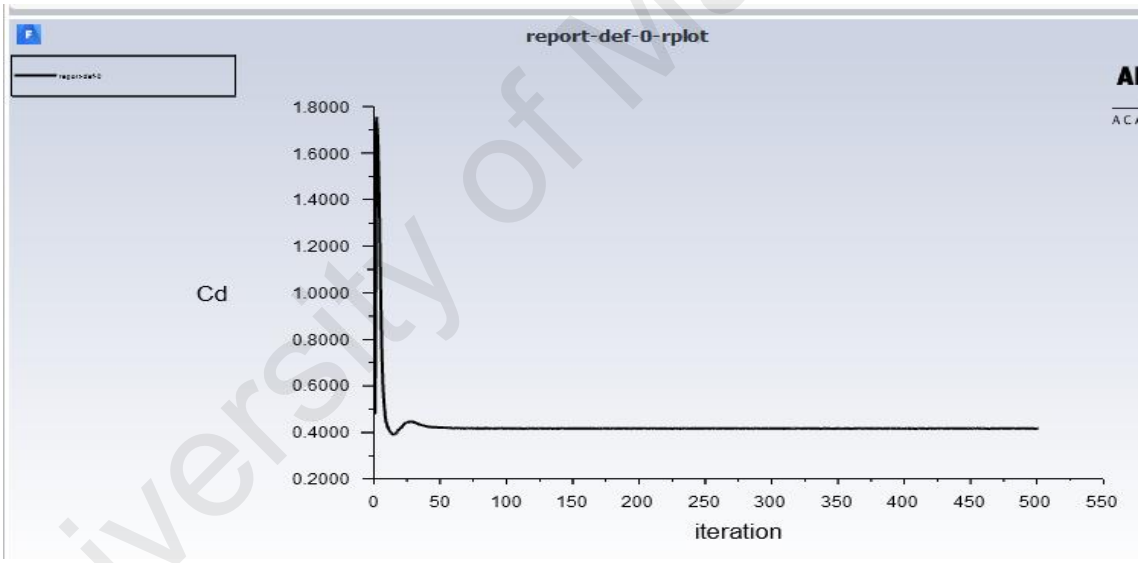


Forces - Direction Vector (-1 0 0)

| | Forces (n) | | | Coefficients | | |
|---|---|---|---|---|---|---|
| Zone | Pressure | Viscous | Total | Pressure | Viscous | Total |
| roof | 1696.3198 | 1127.3987 | 2823.7185 | 0.2503675 | 0.16639786 | 0.41676536 |
| Net | 1696.3198 | 1127.3987 | 2823.7185 | 0.2503675 | 0.16639786 | 0.41676536 |

## APPENDIX S: Residual Scales, drag coefficient & force for model C at 140 Km/h

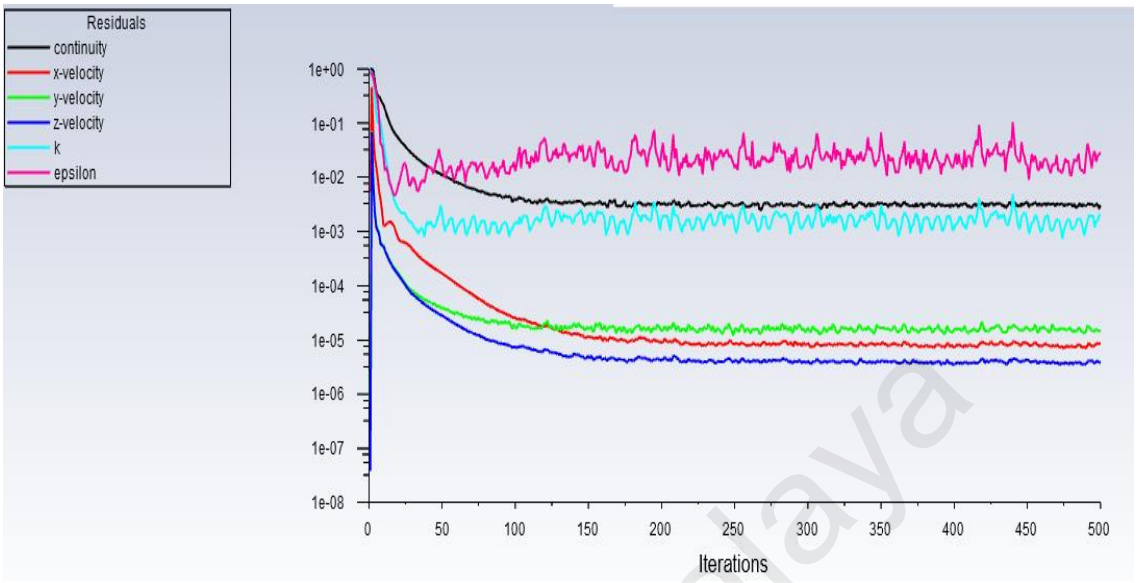


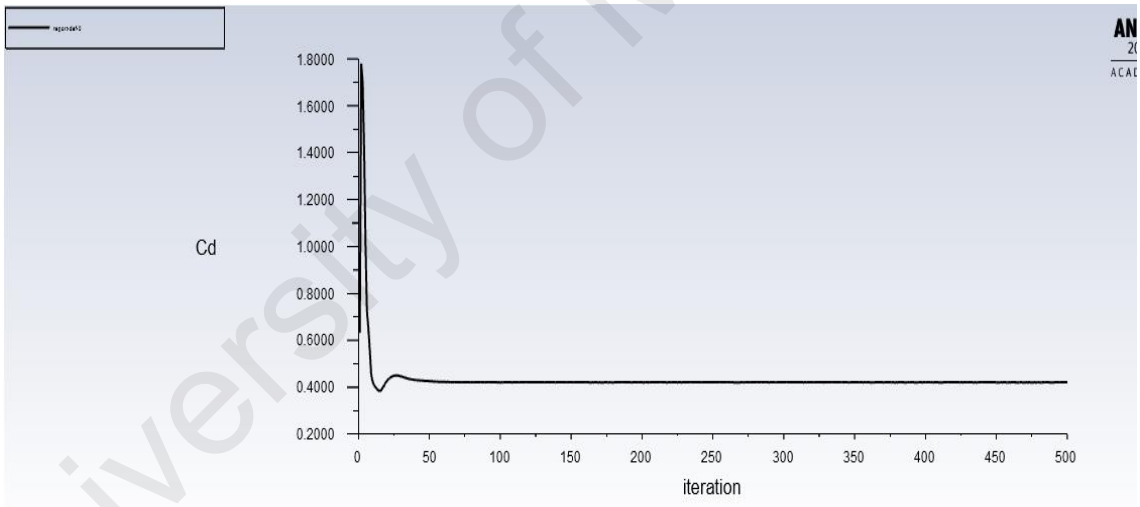


Forces - Direction Vector (-1 0 0)

| | Forces (n) | | | Coefficients | | |
|---|---|---|---|---|---|---|
| Zone | Pressure | Viscous | Total | Pressure | Viscous | Total |
| roof | 1302.0447 | 882.01288 | 2184.0576 | 0.25100364 | 0.17003137 | 0.42103501 |
| Net | 1302.0447 | 882.01288 | 2184.0576 | 0.25100364 | 0.17003137 | 0.42103501 |

## APPENDIX T: Residual Scales, drag coefficient & force for model C at 120 Km/h

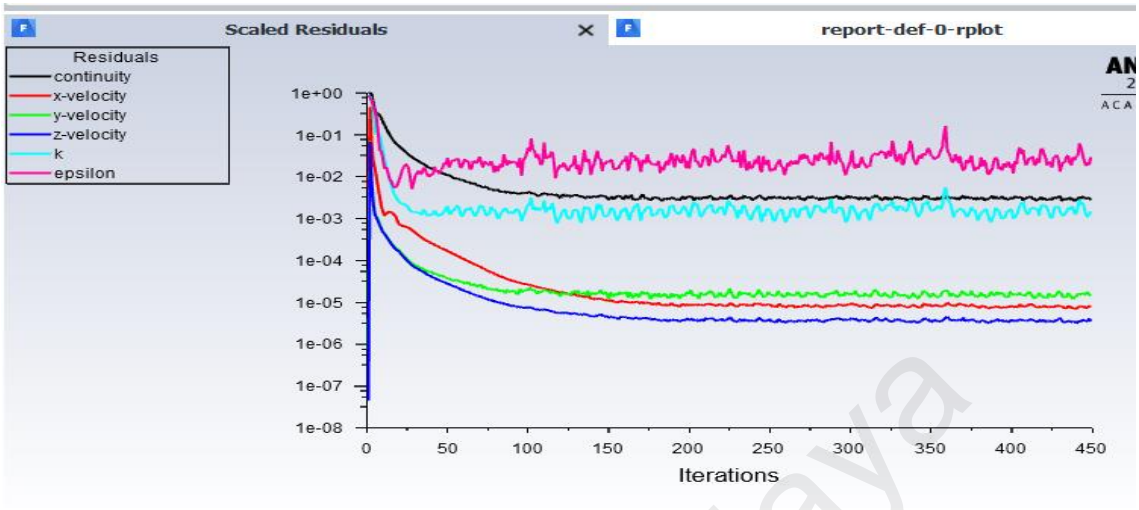


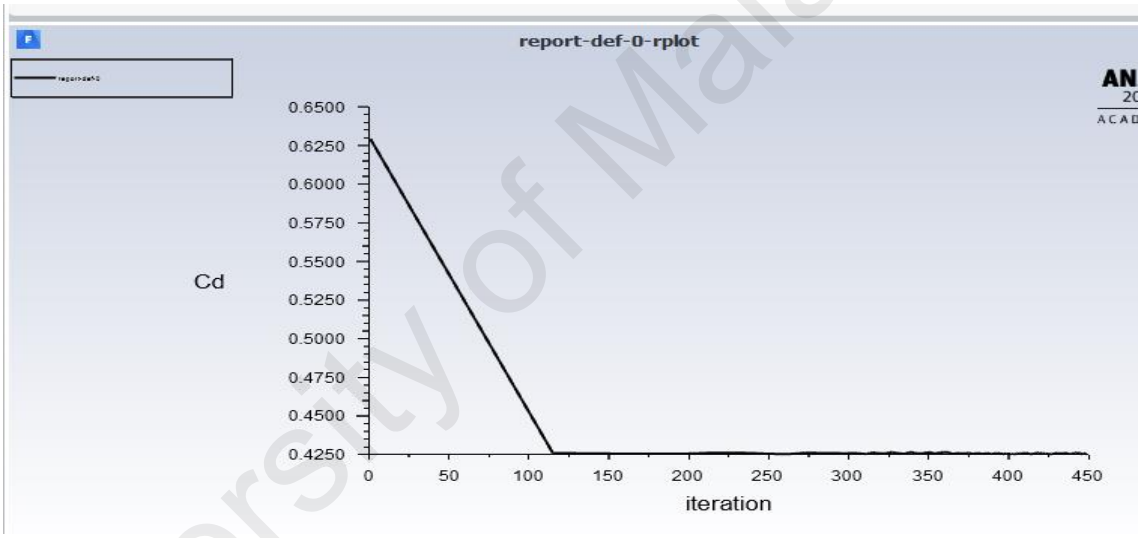


Forces - Direction Vector (-1 0 0)

| | Forces (n) | | | Coefficients | | |
|---|---|---|---|---|---|---|
| Zone | Pressure | Viscous | Total | Pressure | Viscous | Total |
| roof | 959.224 | 662.24731 | 1621.4713 | 0.25169105 | 0.17376725 | 0.4254583 |
| Net | 959.224 | 662.24731 | 1621.4713 | 0.25169105 | 0.17376725 | 0.4254583 |

## APPENDIX U: Residual Scales, drag coefficient & force for model C at 100 Km/h

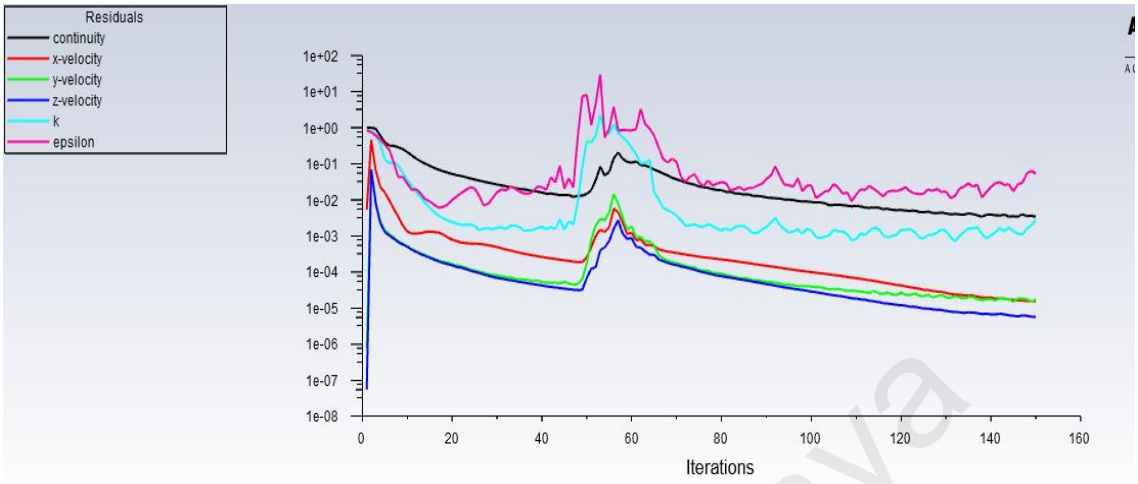


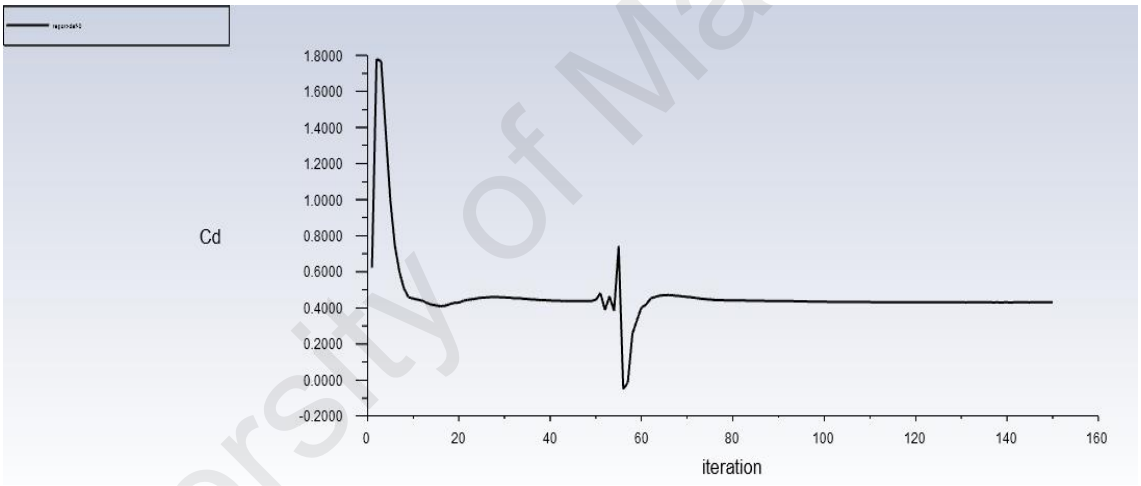


Forces - Direction Vector (-1 0 0)

| | Forces (n) | | | Coefficients | | |
|---|---|---|---|---|---|---|
| Zone | Pressure | Viscous | Total | Pressure | Viscous | Total |
| roof | 668.53937 | 474.07532 | 1142.6147 | 0.25260224 | 0.17912556 | 0.43172779 |
| Net | 668.53937 | 474.07532 | 1142.6147 | 0.25260224 | 0.17912556 | 0.43172779 |

## APPENDIX V: Pressure contour and details for original design at 160Km/h

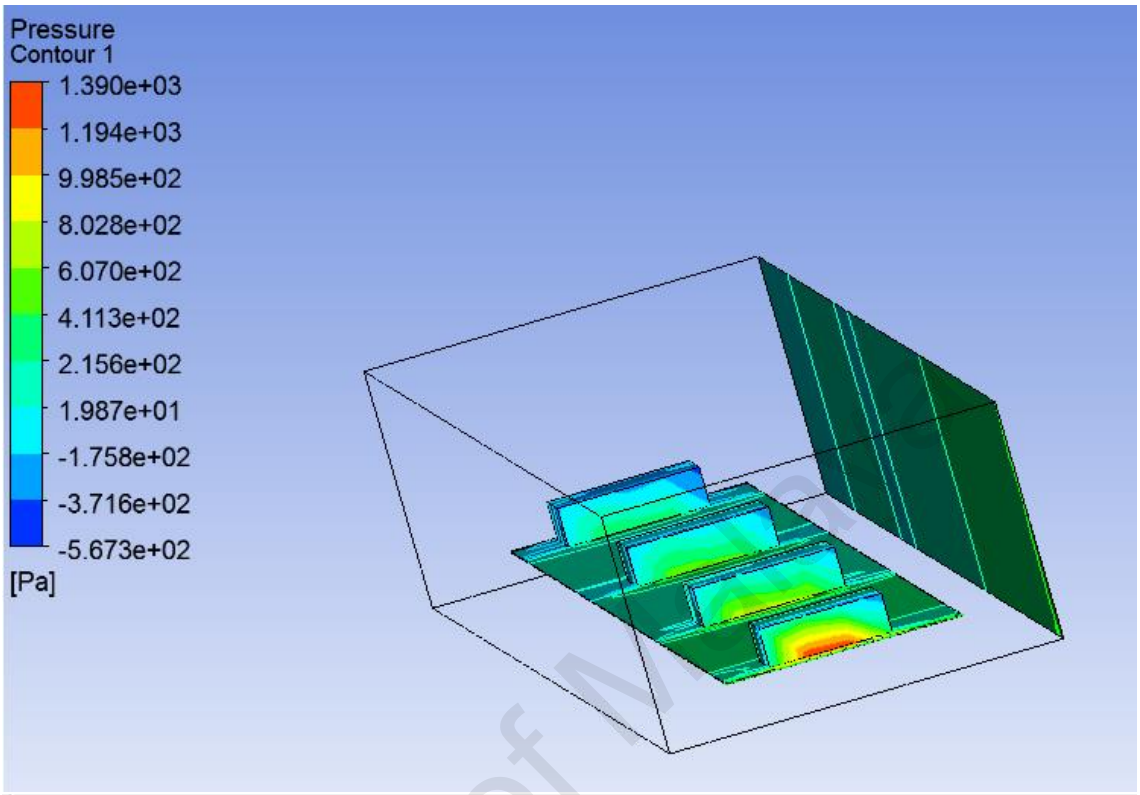


Details of **Contour 1**

| Geometry | Labels | Render | View |
|---|---|---|---|

| | | |
|---|---|---|
| Domains | All Domains | ... |
| Locations | roof | ... |
| Variable | Pressure | ... |
| Range | Global | |
| Min | -567.293 [Pa] | |
| Max | 1389.93 [Pa] | |
| # of Contours | 11 | |

## APPENDIX W: Pressure contour and details for model A at 160Km/h

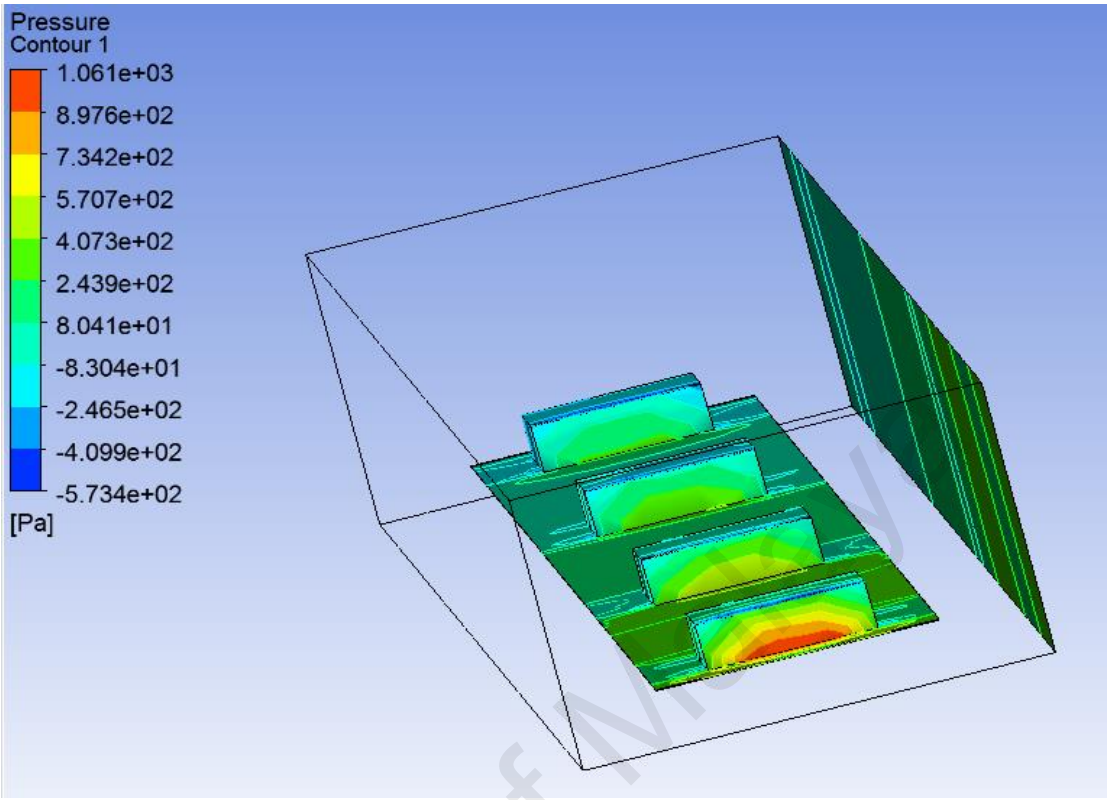


Details of **Contour 1**

| Geometry | Labels | Render | View |
|---|---|---|---|

| | | |
|---|---|---|
| Domains | All Domains | ... |
| Locations | roof | ... |
| Variable | Pressure | ... |
| Range | Global | |
| Min | -573.37 [Pa] | |
| Max | 1061.08 [Pa] | |
| # of Contours | 11 | |

**APPENDIX X: Pressure contour and details for model B at 160Km/h**

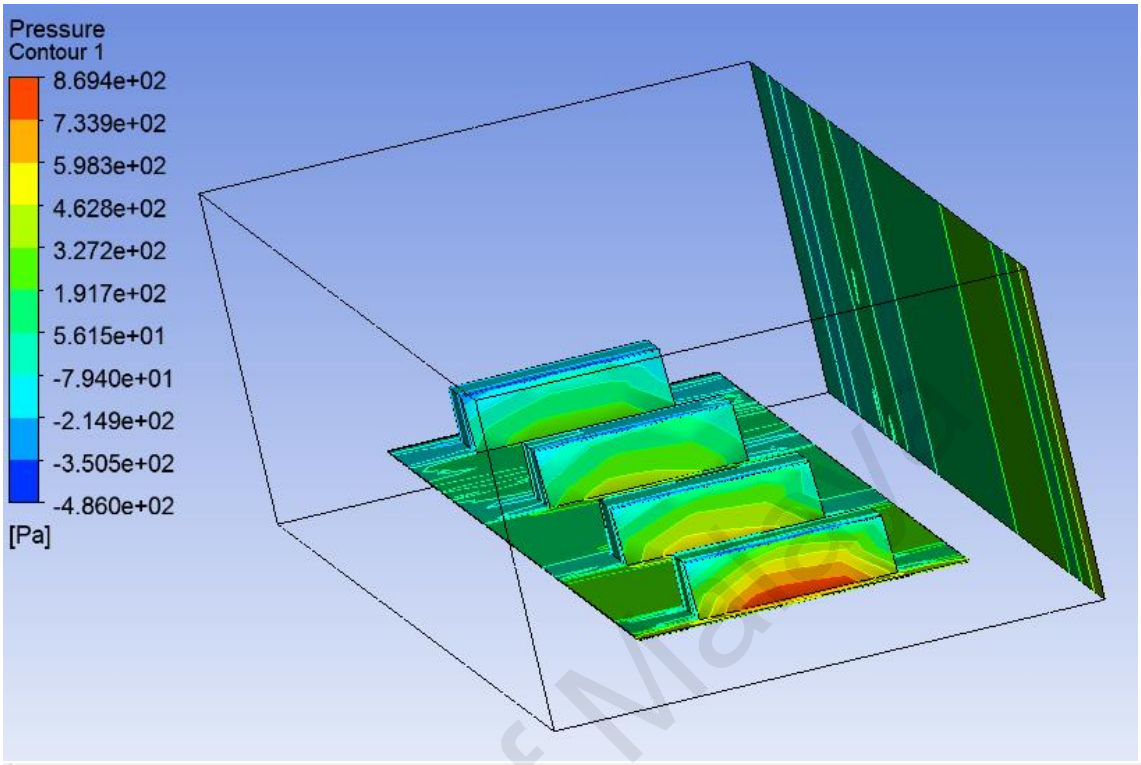


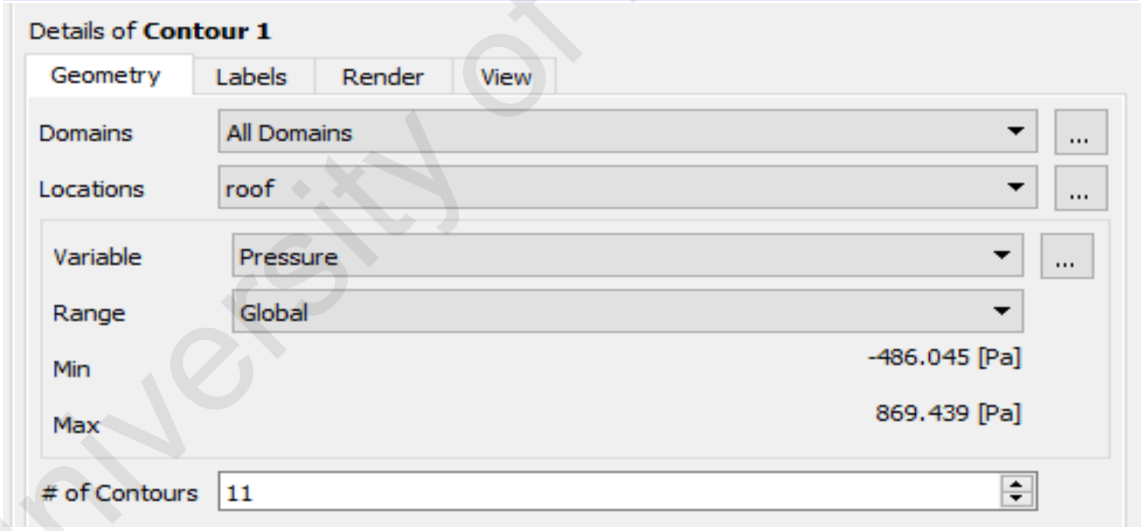

## APPENDIX Y: Pressure contour and details for model C at 160Km/h

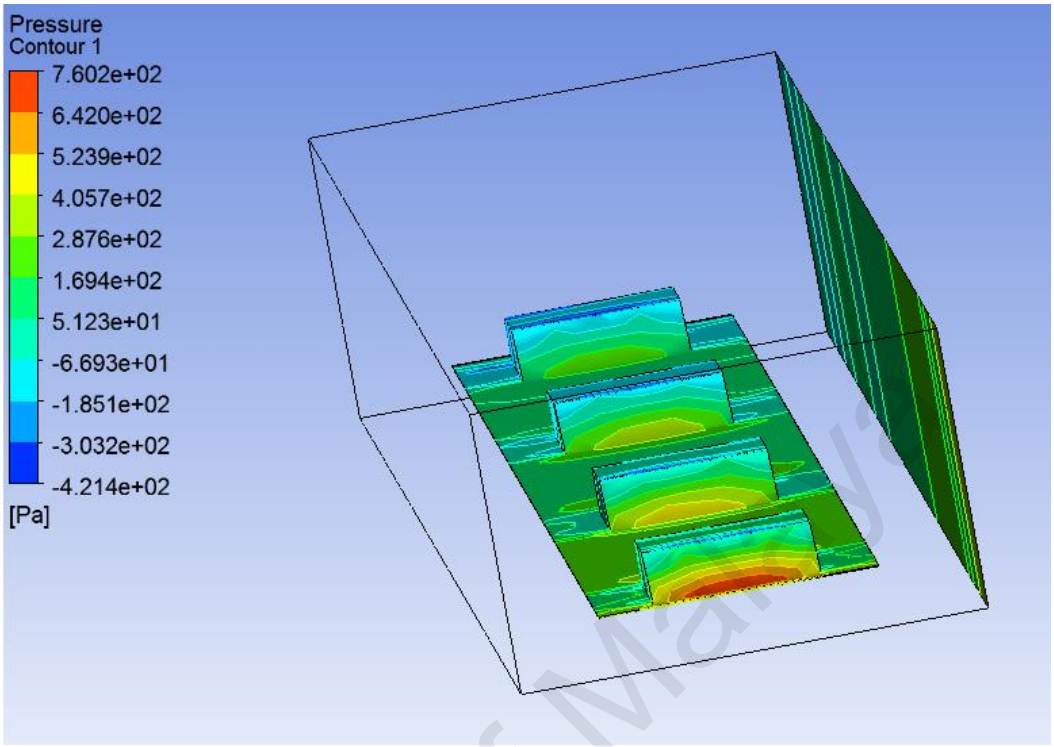


Details of **Contour 1**

| Geometry | Labels | Render | View |
|---|---|---|---|

| | | |
|---|---|---|
| Domains | All Domains | ... |
| Locations | roof | ... |
| Variable | Pressure | ... |
| Range | Global | |
| Min | -421.404 [Pa] | |
| Max | 760.191 [Pa] | |
| # of Contours | 11 | |
| Advanced Properties | | |